ChemPubSoc Europe

DOI: 10.1002/ejic.201901068

EurJIC European Journal of Inorganic Chemistry

Full Paper

Phospholanes

Oligodentate Phosphine Ligands with Phospholane End Groups: New Synthetic Access and Application to Molybdenum-Based Synthetic Nitrogen Fixation

Mareike Pfeil,[a] Tobias A. Engesser,[a] Alexander Koch,[a] Jannik Junge,[a] Jan Krahmer,[a] Christian Näther,[a] and Felix Tuczek*[a]

Abstract: A new synthetic access to oligodentate phosphine ligands with phospholane end groups, starting from lithium phospholanide, is established. Based on this building block, the tridentate ligand **prPP(Ph)P-pln** was synthesized and used for the synthesis of [MoX_3{prPP(Ph)P-pln}] (X = Cl, Br, I) precursors. Sodium amalgam reduction in the presence of N_2 and either mono- or bidentate ligands leads to several molybdenum(0) mono- and bis(dinitrogen) complexes, respectively. With the diphosphine dppm a mixture of *facial* and *meridional* isomers of [$Mo(N_2)${prPP(Ph)P-pln}(dppm)] is formed. Using the monophosphines $PMePh_2$ and PMe_2Ph *mer*-[$Mo(N_2)${prPP(Ph)P-pln}-($PMe_2Ph)_2$] and *trans*-[$Mo(N_2)_2${prPP(Ph)P-pln}($PMePh_2$)] could be obtained. The spectroscopic properties and reactivity of the latter towards protonation was investigated, and a hydrazido complex could be obtained and characterized.

Introduction

Since the discovery of the first dinitrogen complex,[1] the activation and (catalytic) conversion of highly inert dinitrogen into ammonia has been one of the most demanding tasks in bioinorganic and organometallic chemistry.[2] In nature, this reaction is catalyzed by the enzyme nitrogenase,[3] possessing the FeMo cofactor as active site.[4] In the last decades, cyclic and catalytic systems based on transition-metal complexes were developed to mimic this process.[5–10] In the field of synthetic nitrogen fixation, molybdenum-phosphine complexes have been exceedingly successful. The first molybdenum dinitrogen complex supported by phosphine ligands, [$Mo(N_2)_2(dppe)_2$], was synthesized by Hidai et al. already in 1969,[11] and a few years later, Chatt et al. achieved the first (non-catalytic) conversion of dinitrogen into ammonia using complexes of the type [$M(N_2)_2(PR_3)_4$] (M = W or Mo, PR_3 = PMe_2Ph or $PMePh_2$).[10] In the meantime, highly active catalysts have been developed for the N_2-to-NH_3 conversion, some of which are based on molybdenum centers[7,9,12–18] and/or phosphine ligands,[6,7,13–22] although other metals and ligands have been found to be effective as well.[5,6,9,19,21–23]

In the last years, our working group has investigated molybdenum dinitrogen complexes supported by oligodentate phosphine ligands (Figure 1). In order to increase the activation of dinitrogen aryl phosphines were replaced by alkyl phosphines which are better σ donors and weaker π acceptors.[24–29]

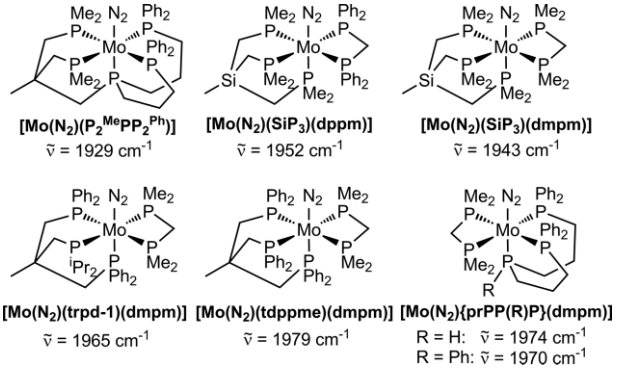

Figure 1. Selected molybdenum(0) dinitrogen complexes synthesized by our working group and corresponding NN stretching frequencies.[24,25,27–30]

However, besides the electronic properties of the phosphine donor groups, also the steric demand of their substituents has to be taken into account.[25,26] Originally, we developed oligodentate ligand systems with diisopropylphosphine end groups, which turned out to be sterically too demanding for certain applications.[25] In order to reduce steric bulk, we introduced smaller substituents like methyl groups.[26–28] On the other hand, experimental evidence exists that a certain degree of shielding is beneficial to enhance the stability of the N_2 ligand and its protonated derivatives.[27,31] With these considerations in mind we decided to explore the use of phospholane donor groups as potentially suitable candidates to combine steric

[a] *Institute of Inorganic Chemistry, Christian-Albrechts University Kiel, Max-Eyth-Strasse 2, 24118 Kiel, Germany*
E-mail: ftuczek@ac.uni-kiel.de
http://www.ac.uni-kiel.de/tuczek

Supporting information and ORCID(s) from the author(s) for this article are available on the WWW under https://doi.org/10.1002/ejic.201901068.

shielding with the high donor strength of alkylphosphines.[25,32,33]

In the literature, phospholane ligands have mostly been investigated in the field of asymmetric catalysis.[34] Ruthenium and rhodium catalysts based on chiral bisphospholane ligands, especially those belonging to the BPE or DuPHOS family,[34,35] first published by Burk et al.,[36,37] have been well explored regarding the enantioselective hydrogenation of unsaturated substrates.[34,38] Other ligand systems like tripodal or tridentate PPP,[37,39] NP_2,[40,41] NP_3,[39–41] as well as PCP[42] or PNP[37,43–45] pincer ligands have been developed. In the last decade, the coordination of asymmetric phospholane ligands to metal centers like Pd(0),[46] Pd(II),[44] Ni(II),[44] Mn(I),[45,47] and Au(I)[41] has become increasingly important. In comparison to chiral phospholanes, the synthesis of achiral ligands containing phospholane groups and their coordination to transition metals is less explored. Only few examples of bisphospholane ligands coordinating to Fe(II),[48] Au(I),[49] Ag(I),[50] or Cu(I)[51] exist. Interestingly, the coordination of phospholane donor groups to molybdenum is almost unknown. To the best of our knowledge, only D'jakonov et al. demonstrated the coordination of monodentate and bidentate phospholane ligands to molybdenum(0) generating two molybdenum(0) carbonyl complexes.[52] In the area of nitrogen fixation, phosphine ligands based on phospholane donor groups have not been studied yet.

Herein, we first present the two-step synthesis of lithium phospholanide (**Li-Pln**) which turned out to be a versatile building block for the synthesis of new non-chiral phospholane containing ligands. As an example for this approach, we describe the synthesis of the non-chiral tridentate ligand bis(3-phospholanopropyl)phenylphosphine [**prPP(Ph)P-pln**]. In order to apply this ligand in molybdenum-based synthetic nitrogen fixation, we investigated its coordination behavior to molybdenum(III) centers. The resulting molybdenum(III) precursors are reduced to the corresponding molybdenum(0) mono(dinitrogen) or bis(dinitrogen) complexes. Thereby, we explored the influence of mono- (PMe_2Ph, $PMePh_2$) and bidentate (dppm, dmpm) coligands on the coordination behavior of **prPP(Ph)P-pln** and the activation of dinitrogen in the respective molybdenum(0) complexes.

Results and Discussion

Synthesis of Lithium Phospholanide (Li-Pln)

As we found out, lithium phospholanide provides an easy and versatile route for the introduction of achiral phospholane groups in oligodentate ligand systems. However, as far as we know, isolated lithium phospholanide (**Li-Pln**) has not been synthesized before.

For the preparation of **Li-Pln**, ethyl dichlorophosphate was converted to ethyl phospholanate via a Grignard reaction, following Polniaszek and Foster.[53] The following synthesis of phospholane (**H-Pln**) was effected by the reduction of ethyl phospholanate using $LiAlH_4$ (Scheme 1). Obtained **H-Pln** was purified via distillation (for NMR spectra of isolated **H-Pln** see SI, Figure S1 and S2). However, this air-sensitive and extremely volatile liquid compound is difficult to handle and cannot be stored conveniently. Therefore, after the solvent diethyl ether and the side product ethanol had been removed via distillation, the product **H-Pln** was distilled directly in a solution of *n*-butyllithium in *n*-hexane (2.5 M). The lithium salt of phospholane (**Li-Pln**) was obtained as colorless solid (in 28 % yield) which is much easier to handle than liquid **H-Pln**.

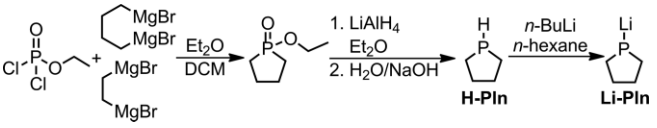

Scheme 1. Synthesis of lithium phospholanide (**Li-Pln**) starting with ethyl phospholanate.

Unexpectedly, more than one signal appears in the $^{31}P\{^1H\}$ NMR spectrum of **Li-Pln** in [D_8]THF (Figure 2, middle). The singlet at –92.1 ppm can be assigned to $P_{Li\text{-}Pln}$, the singlet at –71.0 ppm to $P_{H\text{-}Pln}$[54] and the triplet at –72.8 ppm to the phosphorus $P_{D\text{-}Pln}$ of deuterated phospholane ($^1J_{DP}$ = 28.1 Hz). For **H-Pln** a dm signal with a coupling constant of $^1J_{HP}$ = 180.1 Hz is visible in the proton-coupled ^{31}P NMR spectrum (see SI, Figure S3). The ratio of the $^1J_{HP}$ and $^1J_{DP}$ coupling constants (6.4) is in accordance with the theoretical ratio [$\gamma(H)/\gamma(D) \approx 6.5$]. Furthermore, in the $^{31}P\{^1H\}$ NMR spectrum a singlet appears at –28.3 ppm which is possibly associated with a lithium phospholanide aggregate ($P_{Li\text{-}Pln(aggregate)}$). This signal and the signal at –71.0 ppm ($P_{H\text{-}Pln}$) were found to decrease in intensity if larger amounts of the product **Li-Pln** were dissolved in [D_8]THF (cf. Figure 2, top and middle). To verify the formation of **Li-Pln** aggregates, the ^{31}P NMR spectrum was measured in MeOD. This results in a substitution of lithium by deuterium. As a consequence, only one signal appears that can be assigned to the deuterated phospholane [$P_{D\text{-}Pln}$ = –72.8 ppm (t), cf. Figure 2, bottom]. To investigate if the **Li-Pln** aggregates were formed in the NMR solvent [D_8]THF the product **Li-Pln** was dissolved again in [D_8]THF and 0.1 mL MeOH were added. The solution was investigated via NMR spectroscopy before and after adding

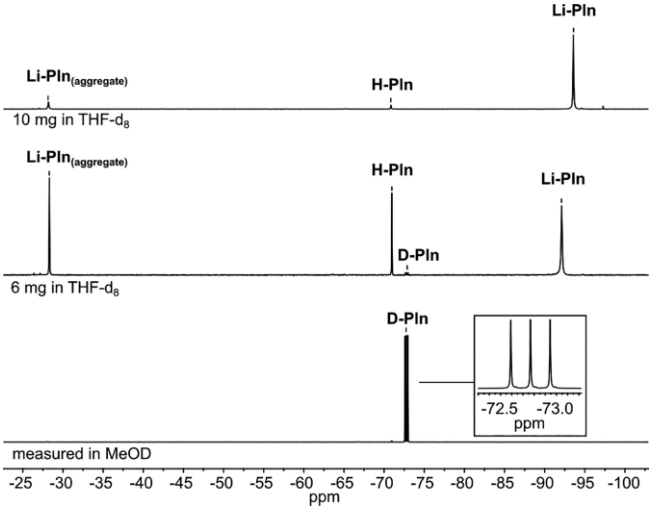

Figure 2. $^{31}P\{^1H\}$ NMR spectra of lithium phospholanide (**Li-Pln**) in [D_8]THF (top, middle) and in MeOD (bottom).

methanol. The signal at –92.1 ppm ($P_{Li\text{-}Pln}$) disappeared, whereas that at –28.3 ppm ($P_{Li\text{-}Pln(aggregate)}$) was still present. Adding higher amounts of MeOH showed no change. These observations indicate that **Li-Pln** in fact is prone to form aggregates in THF, a behavior which is also known from $LiPPh_2$.[55] Additional peaks due to aggregate formation also appear in the ^1H and ^{13}C NMR spectra (NMR spectra see SI, Figure S4 and S5).

Bis(3-phospholanopropyl)phenylphosphine [prPP(Ph)P-pln]

The tridentate ligand **prPP(Ph)P-pln** was synthesized by addition of **Li-Pln** to bis(3-chloropropyl)phenylphosphine in the presence of *n*-butyllithium in THF (Scheme 2).

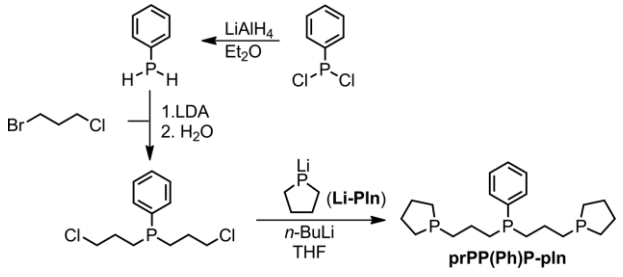

Scheme 2. Synthesis of the tridentate ligand **prPP(Ph)P-pln**.

Starting with the reduction of dichlorophenylphosphine by $LiAlH_4$ as described by Kuchen et al.[56] and Nagel et al.,[57] phenylphosphine as the central building block was obtained. Phenylphosphine was lithiated using lithium diisopropylamide and subsequently converted with 1-bromo-3-chloropropane to bis(3-chloropropyl)phenylphosphine (Scheme 2). This reaction was performed as described by Green and Meek.[58] As the final step, bis(3-chloropropyl)phenylphosphine reacted with **Li-Pln** to form bis(3-phospholanopropyl)phenylphosphine [**prPP(Ph)P-pln**] in an excellent yield (91 %). In order to break up the present **Li-Pln** aggregates (cf. previous section), *n*-BuLi was added to the solution of Li-Pln in THF before adding this mixture to bis(3-chloropropyl)phenylphosphine. This addition is necessary for the complete substitution of the chlorine groups by phospholanide giving the tridentate ligand **prPP(Ph)P-pln** (NMR spectra see SI, Figure S6–S8).

Molybdenum(III) Complexes

In order to obtain information about the coordination behavior of **prPP(Ph)P-pln** to molybdenum centers, the Mo(III) complexes [MoX_3{prPP(Ph)P-pln}] (**1-X**, X = Cl, Br and I) were synthesized according to Scheme 3. These complexes were subsequently reduced to molybdenum(0) dinitrogen complexes (see below).

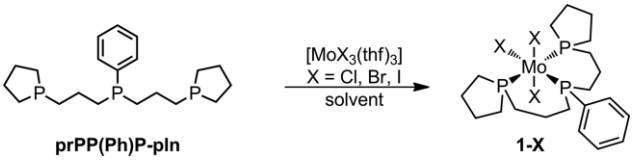

Scheme 3. Synthesis of the molybdenum(III) complexes [MoX_3{prPP(Ph)P-pln}] (**1-X**, X = Cl, Br, I).

Stirring of **prPP(Ph)P-pln** and [$MoX_3(thf)_3$] (**1-X**, X = Cl, Br and I) in THF or in a mixture of THF and dichloromethane for 12 h at room temperature afforded the corresponding molybdenum(III) complexes in reasonable yields (41–74 %). The complexes were characterized by elemental analysis and IR spectroscopy (see Experimental Section). Comparing the FIR spectra of [MoX_3{prPP(Ph)P-pln}] (**1-X**, X = Cl, Br, I; Figure 3) a successive shift of the Mo–X vibrations to lower wavenumbers from [$MoCl_3${prPP(Ph)P-pln}] (**1-Cl**) over [$MoBr_3${prPP(Ph)P-pln}] (**1-Br**) to [MoI_3{prPP(Ph)P-pln}] (**1-I**) is apparent which can be explained by the increasing mass of the halide ligands.

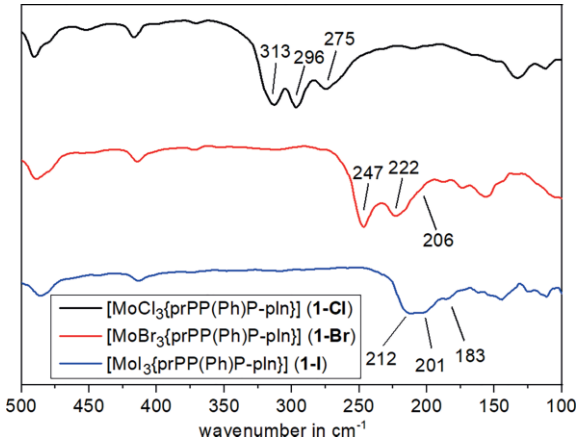

Figure 3. FIR spectra of the molybdenum(III) complexes **1-Cl**, **1-Br** and **1-I**.

Crystals of [$MoCl_3${prPP(Ph)P-pln}] (**1-Cl**) suitable for a X-ray structure determination could be obtained by slow evaporation of the solvent THF and dichloromethane. [$MoCl_3${prPP(Ph)P-pln}] (**1-Cl**) crystallizes in the space group $P2_1/c$ and shows a slightly distorted octahedral coordination geometry whereby the tridentate ligand **prPP(Ph)P-pln** coordinates in a meridional fashion to the molybdenum(III) center (Figure 4). In the literature, only a few crystal structures of molybdenum(III) complexes with the constitution [$MoCl_3$(PPP)] {PPP = $PhP(CH_2CH_2CH_2PPh_2)_2$,[59] $MeP(CH_2CH_2CH_2PMe_2)_2$,[59] $PhP(CH_2CH_2PCy_2)_2$[60] and $P(CH_2CH_2PCy_2)_3$[61]} are known. In these molybdenum(III) complexes the tridentate PPP ligands coordinate meridionally to the molybdenum(III) center as well. To the best of our knowledge, no crystal structure of a molybdenum complex with a phospholane donor group is known so far. The Mo–Cl bond lengths amount to 2.426 Å [Mo–Cl(1)], 2.426 Å [Mo–Cl(2)] and 2.384 Å [Mo–Cl(3)] where Cl(2) and Cl(3) coordinate *trans* to each other. Therefore, it is surprising that the bond lengths [Mo–Cl(2)] and [Mo–Cl(3)] are different whereas the bond lengths of [Mo–Cl(1)] and

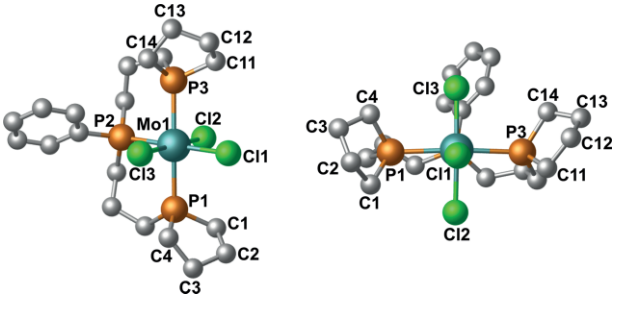

Figure 4. Crystal structure of [$MoCl_3${prPP(Ph)P-pln}] (**1-Cl**), shown in two different perspectives. Hydrogen atoms are omitted for clarity.

[Mo–Cl(2)] are similar. A possible explanation could be the stronger steric influence of the phenyl ring of the tridentate ligand on Cl(3) as compared to Cl(2) (Figure 4, right). The same effect was observed for the complexes of the type $[MoCl_3(PPP)]$ with PPP = $PhP(CH_2CH_2CH_2PPh_2)_2$[59] or $PhP(CH_2CH_2PCy_2)_2$.[60]

Of particular interest are the conformation(s) and bond lengths of the phospholane groups. Both phospholane rings exhibit an envelope conformation meaning that in each case one carbon atom stands out of the ring plane [*endo* position: C(3) and C(13)]. The bond lengths P(3)–C(14) (1.842 Å) and P(3)–C(11) (1.843 Å) are nearly identical, whereas the bond lengths P(1)–C(1) (1.846 Å) and P(1)–C(4) (1.831 Å) differ from each other. Also the bond lengths C(1)–C(2) (1.557 Å) and C(3)–C(4) (1.518 Å) differ more from each other than the bond lengths C(11)–C(12) (1.511 Å) and C(13)–C(14) (1.524 Å). Again, the small differences between both phospholane rings may be caused by the steric influence of the phenyl ring.

Synthesis of Dinitrogen Complexes Containing the Tridentate Ligand prPP(Ph)P-pln

To gain insight into the ability of the molybdenum(0) complexes supported by **prPP(Ph)P-pln** to bind and activate dinitrogen, the molybdenum(III) precursors **1-Br** and **1-I** were reduced by sodium amalgam in the presence of monodentate ($PMePh_2$, PMe_2Ph) or bidentate phosphine coligands (dppm, dmpm). Because the molybdenum(III) complex **1-Cl** was obtained with much lower yield in comparison to **1-Br** and **1-I**, this precursor was not used for the sodium amalgam reductions. The results are presented in the following sections.

Synthesis of Molybdenum(0) Dinitrogen Complexes in the Presence of Bidentate Coligands (dppm, dmpm)

For the synthesis of a molybdenum(0) dinitrogen complex $[MoI_3\{prPP(Ph)P\text{-}pln\}]$ (**1-I**) and one equivalent of dppm [bis(diphenylphosphino)methane] as coligand were stirred with sodium amalgam in THF for 12 h (Scheme 4). The reaction product was highly sensitive to vacuum and could not be precipitated by addition of MeOH. Therefore, the solvent was removed by a stream of nitrogen and the obtained sticky oil was characterized by IR and NMR spectroscopy.

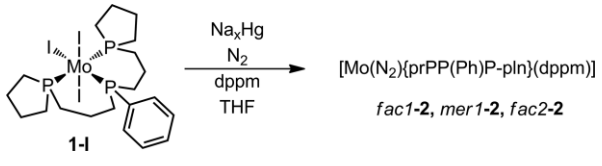

Scheme 4. Sodium amalgam reduction of $[MoI_3\{prPP(Ph)P\text{-}pln\}]$ (**1-I**) with one equivalent dppm. A mixture of isomers (*fac1*-**2**, *mer1*-**2**, *fac2*-**2**) was obtained.

The product exhibits a broad and intense NN stretching band at 1929 cm^{-1} as well as three shoulders at 1955, 1986 and 1997 cm^{-1} (Figure 5). The presence of more than one NN stretching vibration indicates the formation of several complexes. The intense band at 1929 cm^{-1} has the same frequency as the NN stretch of the complex $[Mo(N_2)(P_2{}^{Me}PP_2{}^{Ph})]$ ($\tilde{\nu}$ = 1929 cm^{-1})[27] which to date exhibited the lowest NN stretching frequency of a molybdenum mono(dinitrogen) complex with a pentaphosphine environment.

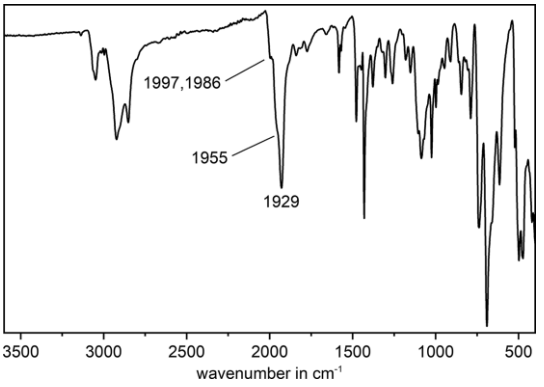

Figure 5. IR (ATR) spectrum of the product of the sodium amalgam reduction of $[MoI_3\{prPP(Ph)P\text{-}pln\}]$ (**1-I**) in the presence of one equivalent dppm.

The ^{31}P NMR spectrum of the product mixture (Figure 6 and S9) shows the formation of the three isomeric molybdenum(0) dinitrogen complexes, *fac1*-$[Mo(N_2)\{prPP(Ph)P\text{-}pln\}(dppm)]$ (*fac1*-**2**) (Figure 6, blue), *mer1*-$[Mo(N_2)\{prPP(Ph)P\text{-}pln\}(dppm)]$ (*mer1*-**2**) (red) and *fac2*-$[Mo(N_2)\{prPP(Ph)P\text{-}pln\}(dppm)]$ (*fac2*-**2**) (green), which exist in a ratio of 10:6:1. The remaining signals belong to free ligands and a side product (*) which is possibly $[Mo(dppm)_3]$[62] (see below).

The molybdenum-containing isomers and signals could be assigned on the basis of ^{31}P-, $^{31}P,^{31}P$-COSY- and $^{1}H,^{31}P$-HMBC-NMR spectra (Figure S10 and S11). For the isomer *fac1*-$[Mo(N_2)\{prPP(Ph)P\text{-}pln\}(dppm)]$ (*fac1*-**2**) a set of four dddd-signals located at 31.9, 27.2, 12.7, 10.3 ppm, and one pseudo-"dtd" signal at 19.5 ppm appear in the ^{31}P NMR spectrum (Figure 6, blue). The coupling between these P nuclei can be observed in the $^{31}P,^{31}P$-COSY NMR spectrum (Figure S10). The signal at 31.9 ppm is assigned to the equatorial phospholane P atom (P_a) and the signal at 27.2 ppm to the axial phospholane P atom (P_b) which is coordinated to the molybdenum center in *trans* position to the N_2 ligand. The latter assignment is also supported by a missing large coupling constant in the range of 90–110 Hz. The pseudo-"dtd"-signal at 19.5 ppm can be assigned to the central P atom P_d of **prPP(Ph)P-pln**. The coupling constants between P_d and P_g or P_a ($^2J_{PP}$ = 27.8 and 27.7 Hz) are nearly identical leading to the observed pseudo-"dtd" instead of a "dddd" pattern. The signal at 12.7 ppm is attributed to P_g, the PPh_2 group of the coligand dppm which is in *trans* position to the phospholane P atom P_a ($^2J_{PaPg}$ = 95.7 Hz). Finally, the signal at 10.3 ppm is assigned to P_h, the PPh_2 group of the coligand which coordinates *trans* to the central ligand P atom P_d ($^2J_{PdPh}$ = 91.3 Hz).

For the isomer *mer1*-$[Mo(N_2)\{prPP(Ph)P\text{-}pln\}(dppm)]$ (*mer1*-**2**) a set of two dddd-signals located at 22.0 and 17.9 ppm and two dtd-signals located at 13.3 and 4.5 ppm are observed in the ^{31}P NMR spectrum (Figure 6, red). The coupling of these P nuclei among each other is shown in the $^{31}P,^{31}P$-COSY NMR spectrum (Figure S10). The signal at 22.0 ppm can be assigned to both phospholane nuclei P_c and $P_{c'}$ which coordinate *trans* to each other. Of course, magnetically equivalent phosphorus

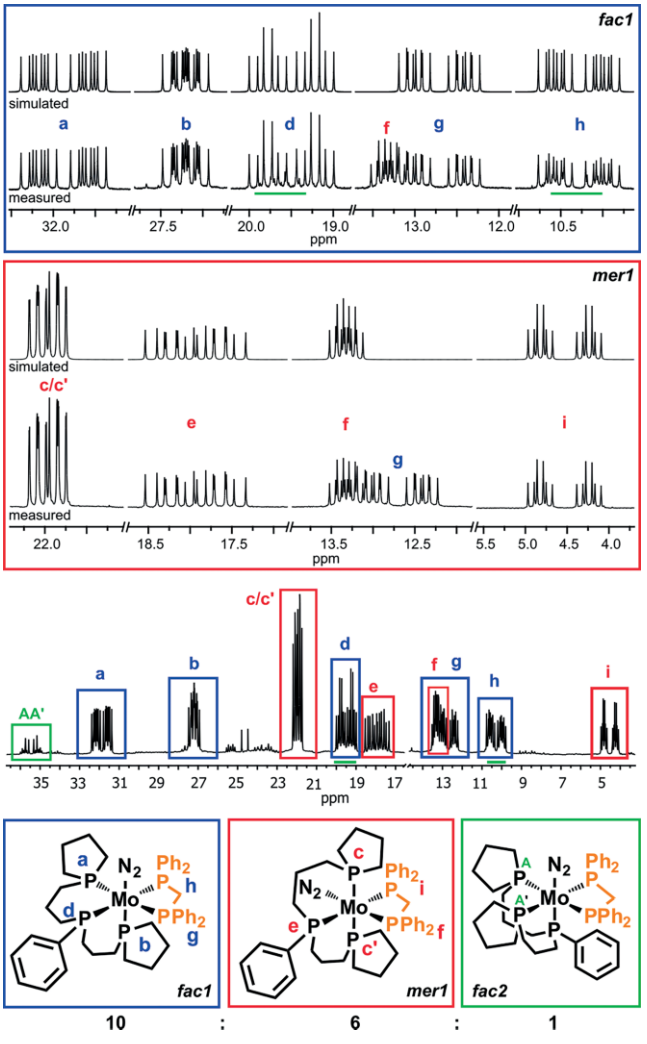

Figure 6. $^{31}P\{^{1}H\}$ NMR spectrum of [Mo(N_2){prPP(Ph)P-pln}(dppm)] (**2**) measured in C_6D_6: Bottom: Structure formulae; middle: $^{31}P\{^{1}H\}$ NMR spectrum between 36 ppm and 4 ppm; top: comparison of the measured and simulated spectra for the ***fac1***- and ***mer1***-isomer of **2** (enlarged sections).

nuclei are not supposed to show a coupling to each other. Nevertheless, a coupling constant of 1.1 Hz is observable. This behavior can be explained by different conformations of the phospholane rings. Already in the crystal structure of the molybdenum(III) complex [$MoCl_3$}prPP(Ph)P-pln}] (**1-Cl**) different bond lengths within the phospholane rings were observed (see above and Figure 4). The dddd-signal at 17.9 ppm is assigned to the central P atom P_e of the tridentate ligand whereas the dtd-signal at 13.3 ppm is attributed to the PPh_2 group of the coligand dppm that is coordinated in *trans* position to the N_2 ligand (P_f). For the other PPh_2 group of the coligand (P_i) a dtd-signal is observed at 4.5 ppm ($^{2}J_{PePi}$ = 94.5 Hz).

Finally, the ^{31}P NMR spectrum of the product mixture resulting from the sodium amalgam reduction of [MoI_3}prPP(Ph)P-pln}] (**1-I**) in the presence of one equivalent dppm exhibits a third isomer (Figure 6, green), albeit with little intensity. The signal at 35.5 ppm is probably the AA′ part of an AA′XX′M pattern. In the $^{31}P,^{31}P$-COSY NMR spectrum (NMR spectra see SI, Figure S10) a coupling to two other signals is visible, but these signals are hidden by the signals of P_d and P_h of *fac1*-[Mo(N_2){prPP(Ph)P-pln}(dppm)] (*fac1*-**2**). These findings suggest formation of the isomer *fac2*-[Mo(N_2){prPP(Ph)P-pln}(dppm)] (*fac2*-**2**), in which the central P(Ph)-moiety of the tridentate ligand coordinates *trans* to N_2.

DFT calculations show that the ***fac1***- and ***mer1***-isomers, indeed, are more stable than the ***fac2***-isomer, which is present in solution as a minor product (Figure 7). However, the calculated ***mer1***-structure is more stable than the ***fac1***-isomer, in contrast to the experiment where ***fac1*** exhibits the highest concentration. This may reflect a kinetic control of the formation of these complexes, affected by the sterically demanding residues.

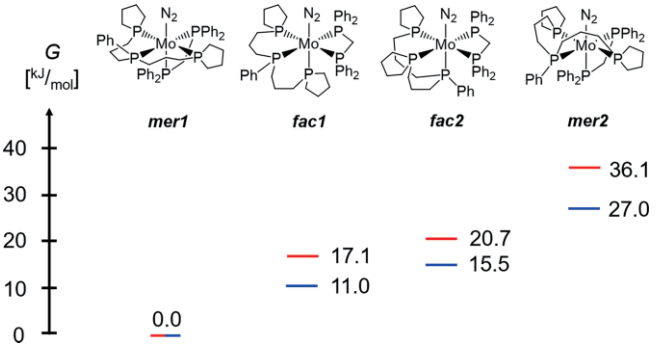

Figure 7. Calculated free energies (B3LYP/def2-TZVPP) of the different isomers of [Mo(N_2){prPP(Ph)P-pln}(dppm)] (**2**) with (blue, D3BJ) and without (red) dispersion correction. (For more details see SI, Figure S25 and S26).

Besides the described molybdenum(0) dinitrogen complexes *fac1*-**2**, *mer1*-**2** and *fac2*-**2** a singlet appears at 15.5 ppm which, according to the $^{1}H,^{31}P$-HMBC spectrum (Figure S11), can be assigned to [Mo(dppm)$_3$].[62] To confirm the formation of [Mo(dppm)$_3$] we reduced [$MoCl_3$(thf)$_3$] in the presence of three equivalents dppm via sodium amalgam according to the literature.[62] The NMR spectra (Figure S12 and S13) and the missing NN stretching vibration in the IR spectrum (Figure S23) support our assumption that [Mo(dppm)$_3$] was formed. However, it is known that the complex [Mo(dppm)$_3$] is labile,[63] which may explain the large amount of dppm (cf. Figure S9 and S12). This also indicates that the formation of a dinitrogen complex supported by the tridentate ligand **prPP(Ph)P-pln** and dppm is not particularly favorable. In order to investigate whether the steric demand of dppm has a negative impact on the formation of [Mo(N_2){prPP(Ph)P-pln}(dppm)] (**2**), dmpm was employed as a coligand. However, no well-defined and stable complexes could be isolated in this case. The ^{31}P NMR spectrum and the calculated free energies of different isomers of the complex [Mo(N_2){prPP(Ph)P-pln}(dmpm)] are given in the SI, Figure S14 and S26, respectively.

Synthesis of Molybdenum(0) Dinitrogen Complexes in the Presence of Monodentate Coligands ($PMePh_2$, PMe_2Ph) and Investigation of their Reactivities towards Acids

To explore whether it is possible to synthesize a molybdenum(0) bis(dinitrogen) complex supported by the tridentate ligand **prPP(Ph)P-pln** [$MoBr_3$}prPP(Ph)P-pln}] (**1-Br**) was subjected to a sodium amalgam reduction in the presence of N_2 and the monodentate ligands $PMePh_2$ and PMe_2Ph which have

different steric demands {**1-Br** turned out to be easier accessible in pure form than [MoI$_3$(prPP(Ph)P-pln)] (**1-I**)}. In the following, the results of these investigations are described in more detail.

Synthesis of [Mo(N$_2$)$_2$(prPP(Ph)P-pln)(PMePh$_2$)] (3)

Employing one equivalent of PMePh$_2$ yielded the bis(dinitrogen) complex *trans*-[Mo(N$_2$)$_2$(prPP(Ph)P-pln)(PMePh$_2$)] (**3**; Scheme 5). The complex could be obtained as an orange-colored solid by precipitation with methanol and was characterized by IR, Raman and NMR spectroscopy as well as by elemental analysis. Employing two equivalents of PMePh$_2$ also afforded **3** along with one equivalent of uncoordinated PMePh$_2$ instead of a mono(dinitrogen) complex (see below). However, it was not possible to precipitate the product in this case.

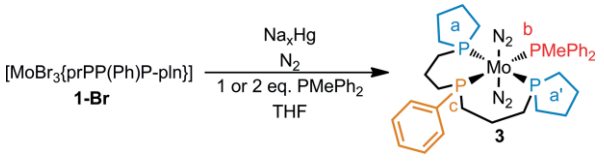

Scheme 5. Synthesis of [Mo(N$_2$)$_2$(prPP(Ph)P-pln)(PMePh$_2$)] (**3**) via sodium amalgam reduction of [MoBr$_3$(prPP(Ph)P-pln)] (**1-Br**) in the presence of one or two equivalent(s) PMePh$_2$.

The IR and Raman spectra of **3** indicate the formation of a *trans*-bis(dinitrogen) complex (Figure 8). Specifically, the IR spectrum shows an intense band at 1924 cm^{-1} which is assigned to the antisymmetric and a small band at 2005 cm^{-1} which is assigned to the symmetric NN stretching vibration of the two N$_2$ ligands. The Raman spectrum exhibits the corresponding bands at 2000 cm^{-1} and 1930 cm^{-1} but with an opposite intensity ratio compared to the IR spectrum.

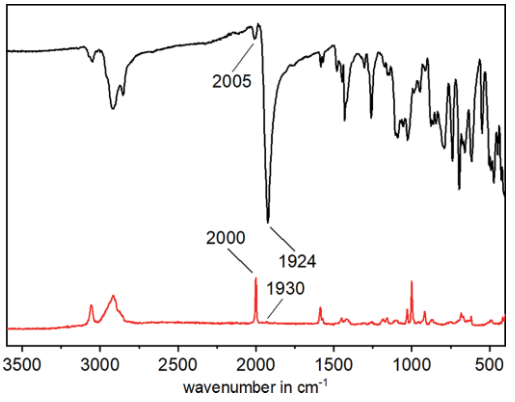

Figure 8. IR (ATR) (top, black) and Raman spectrum (bottom, red) of the bis(dinitrogen) complex [Mo(N$_2$)$_2$(prPP(Ph)P-pln)(PMePh$_2$)] (**3**).

The formation of *trans*-[Mo(N$_2$)$_2$(prPP(Ph)P-pln)(PMePh$_2$)] (**3**) is further supported by ^{31}P NMR spectroscopy (Figure 9, bottom). A set of signals located at 25.0, 22.8 and 18.0 ppm for the *trans*-[Mo(N$_2$)$_2$(prPP(Ph)P-pln)(PMePh$_2$)] complex (**3**) are observed. The signal at 25.0 ppm is assigned to both phospholane P atoms P$_a$ and P$_{a'}$ which are in *trans* position to each other [Figure 9 (bottom), Scheme 5]. For the coordinated coligand PMePh$_2$ a dt-signal pattern at 22.8 ppm is observed [P$_b$, Figure 9

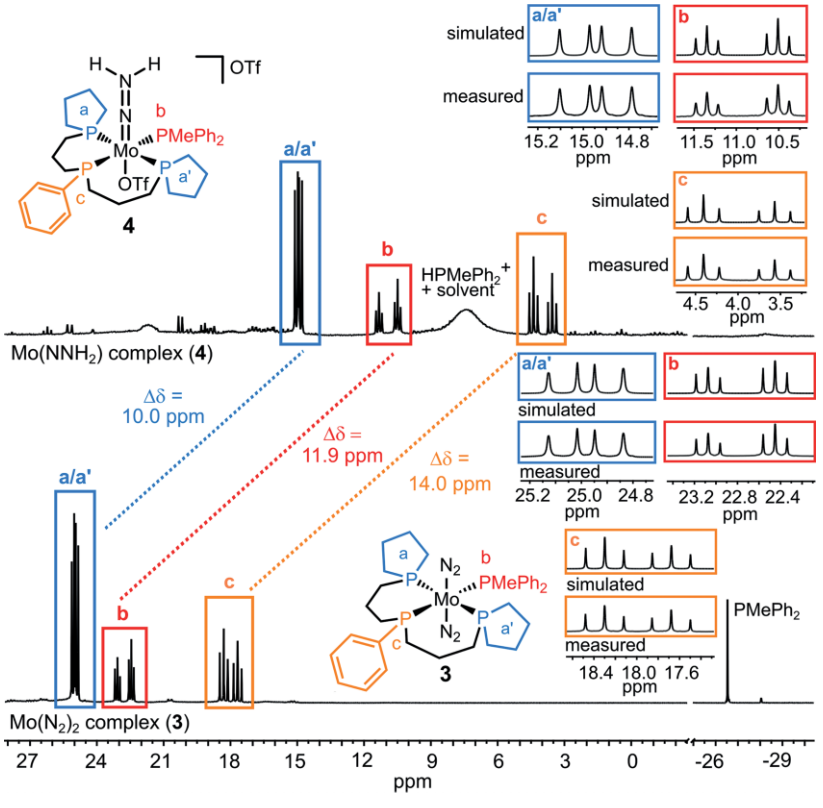

Figure 9. ^{31}P{^{1}H} NMR spectra of [Mo(N$_2$)$_2$(prPP(Ph)P-pln)(PMePh$_2$)] (**3**) measured in [D$_8$]THF (bottom) and [Mo(NNH$_2$)(OTf){prPP(Ph)P-pln}(PMePh$_2$)]OTf (**4**) measured in CD$_2$Cl$_2$ (top). Furthermore, enlarged signals (measured and simulated) of the complexes **3** and **4** are shown. Full ^{31}P NMR spectra see SI (Figure S15 and S17).

(bottom), Scheme 5]. The central PPh group of **prPP(Ph)P-pln** (P_c) coordinates in *trans* position to $PMePh_2$ (P_b) and gives rise to a dt-signal at 18.0 ppm [Figure 9 (bottom), Scheme 5]. Furthermore, a large *trans* coupling between the central PPh (P_c) and $PMePh_2$ (P_b) is observed ($^2J_{PbPc}$ = 100.8 Hz).

Synthesis of [Mo(NNH$_2$)(OTf){prPP(Ph)P-pln}(PMePh$_2$)]OTf (4)

The formation of a hydrazido complex by protonation of bis(dinitrogen) complexes represents the first step towards the generation of ammonia (Chatt cycle).[10,64] In fact, conversion of the bis(dinitrogen) complex [Mo(N$_2$)$_2${prPP(Ph)P-pln}(PMePh$_2$)] (**3**) to the hydrazido complex [Mo(NNH$_2$)(OTf){prPP(Ph)P-pln}(PMePh$_2$)]OTf (**4**) could be effected by addition of triflic acid (TfOH) in a NMR experiment performed in [D$_{10}$]Et$_2$O and CD$_2$Cl$_2$.

The orange-colored bis(dinitrogen) complex **3** was dissolved in [D$_{10}$]Et$_2$O and 2.5 equivalents of TfOH were added, leading to precipitation of a grey solid. The solvent was removed in vacuo and the solid was dissolved in CD$_2$Cl$_2$ whereby the solution became red. After the addition of the acid NMR spectra were measured immediately. The $^{31}P\{^1H\}$ NMR spectrum proves the retention of the tetraphosphine ligand sphere. Compared to the bis(dinitrogen) complex [Mo(N$_2$)$_2${prPP(Ph)P-pln}(PMePh$_2$)] (**3**) all signals are shifted to higher field by 10 – 14 ppm (cf. Figure 9). The signal of the phospholane P atoms P_a and $P_{a'}$ of complex **4** appears at 15.0 ppm whereby the signal of the coordinated coligand $PMePh_2$ (P_b) can be found at 10.9 ppm. The signal of the P(Ph) group (P_c) of the tridentate ligand **prPP(Ph)P-pln** has been shifted to 4.00 ppm. Moreover, the *trans*-coupling constant of the P nuclei P_b and P_c ($^2J_{PbPc}$ = 135.6 Hz) has significantly been increased by the formation of the hydrazido complex **4**.

The ^1H NMR spectrum of the solution after protonation reveals a singlet at 8.9 ppm that corresponds to the NNH$_2$ protons (Figure S18). In the ^{19}F NMR spectrum one intense singlet at –79.3 ppm associated with the fluorine atoms of TfO$^-$ is visible (Figure S19). It seems that ligand exchange occurs between coordinated and solvated TfO$^-$ at a temperature of 300 K.

After removing the solvent from the protonation solution an IR spectrum [Figure 10, red (bottom)] was measured from the obtained yellow oil. No bands for the NN-vibrations of [Mo(N$_2$)$_2${prPP(Ph)P-pln}(PMePh$_2$)] (**3**) are visible. However, the IR spectrum shows two weak bands at 3246 and 3103 cm^{-1} which can be assigned to the NH stretching vibrations of the NNH$_2$ group.

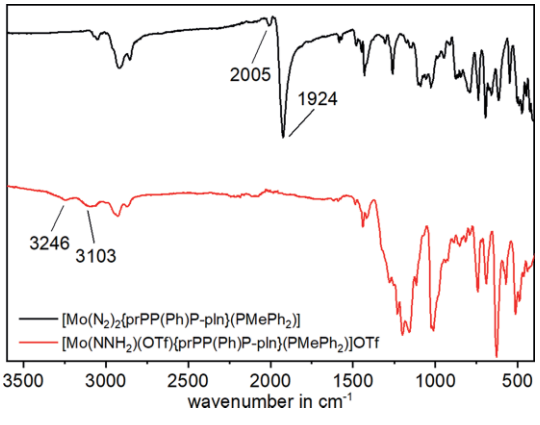

Figure 10. Comparison of the IR (ATR) spectra of [Mo(N$_2$)$_2${prPP(Ph)P-pln}(PMePh$_2$)] (**3**) (black, top) and [Mo(NNH$_2$)(OTf){prPP(Ph)P-pln}(PMePh$_2$)]OTf (**4**) (red, bottom).

Synthesis of [Mo(N$_2$){prPP(Ph)P-pln}(PMe$_2$Ph)$_2$] (5)

In order to investigate whether formation of the bis(dinitrogen) complex [Mo(N$_2$)$_2${prPP(Ph)P-pln}(PMePh$_2$)] (**3**) is influenced by the steric demand of the monophosphine, we also employed PMe_2Ph as a coligand which exhibits a smaller Tolman cone angle (122°)[33] than $PMePh_2$ (136°).[33] If the sodium amalgam reduction of [MoBr$_3${prPP(Ph)P-pln}] (**1-Br**) was performed in the presence of two equivalents of the monophosphine PMe_2Ph, the mono(dinitrogen) complex [Mo(N$_2${prPP(Ph)P-pln}(PMe$_2$Ph)$_2$] (**5**) was obtained (Scheme 6). Using one equivalent of PMe_2Ph did not lead to the corresponding bis(dinitrogen) complex, but to the mono(dinitrogen) complex **5** as well; however, not in a pure form.

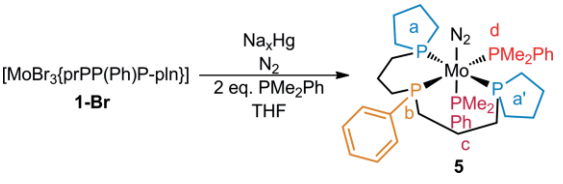

Scheme 6. Synthesis of the mono(dinitrogen) complex [Mo(N$_2${prPP(Ph)P-pln}(PMe$_2$Ph)$_2$] (**5**) via sodium amalgam reduction of [MoBr$_3${prPP(Ph)P-pln}] (**1-Br**) in the presence of two equivalents PMe_2Ph.

By precipitation with MeOH **5** could be isolated as a red solid. The corresponding IR spectrum (Figure 11, top, black) exhibits an intense NN stretching band at 1931 cm^{-1} and a shoulder at 1944 cm^{-1} whereas the Raman spectrum exhibits a strong peak at 1944 cm^{-1} and a smaller one at 1933 cm^{-1} (Figure 11, bottom, red). In contrast to the bulk, the liquid IR spectrum reveals only one broad NN stretching band at 1945 cm^{-1} (Liquid IR spectrum see SI, Figure S24). The absence of the shoulder in the liquid IR reveals that the second band is due the solid state effect (Davydov splitting).[65]

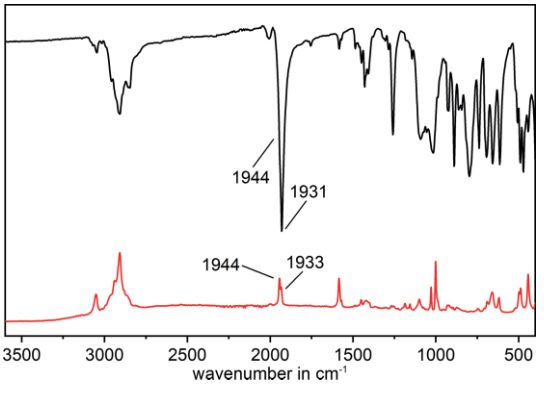

Figure 11. IR (ATR) (black, top) and Raman (red, bottom) spectrum of [Mo(N$_2${prPP(Ph)P-pln}(PMe$_2$Ph)$_2$] (**5**).

The ^{31}P NMR spectrum of [Mo(N$_2${prPP(Ph)P-pln}(PMe$_2$Ph)$_2$] (**5**; cf. Figure 12; full spectrum see SI, Figure S20) proves that only one complex is formed; i.e., the spectrum exhibits a set of four signals relating to the mono(dinitrogen) complex **5** and a

singlet relating to a small amount of uncoordinated coligand PMe_2Ph.

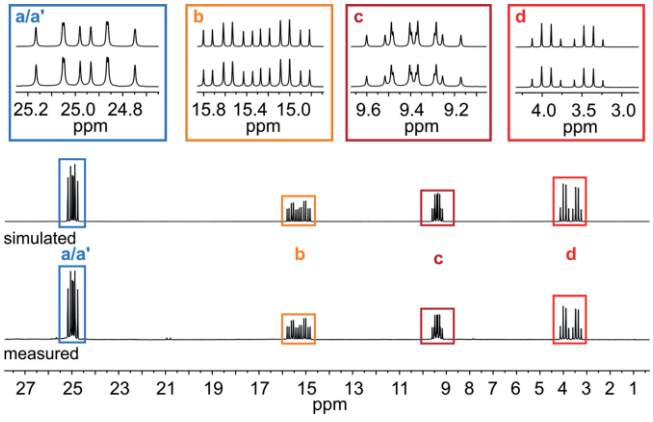

Figure 12. Measured and simulated ^{31}P NMR spectra of [Mo(N_2){prPP(Ph)P-pln}(PMe_2Ph)$_2$] (**5**).

A ddd-signal pattern located at 25.0 ppm can be assigned to the two phospholane P atoms P_a and $P_{a'}$ which are in *trans* position to each other (Figure 12, Scheme 6). In comparison to the complex *mer1*-[Mo(N_2){prPP(Ph)P-pln}(dppm)] (*mer1*-**2**) the ^{31}P nuclei of both phospholanes seem to be magnetically equivalent as no *trans* coupling is visible. The dtd-signal at 15.3 ppm can be assigned to the central P(Ph) group of the tridentate ligand **prPP(Ph)P-pln** (P_b, Figure 12, Scheme 6). One coligand PMe_2Ph (P_d) is coordinated *trans* to P_b ($^2J_{PbPd}$ = 85.9 Hz). The corresponding signal is located at 3.7 ppm and exhibits a dtd-signal pattern. The second coligand PMe_2Ph (P_c, Scheme 6), which coordinates *trans* to N_2, gives rise to a dtd-signal at 9.4 ppm (Figure 12). Unfortunately, the elemental analysis of [Mo(N_2){prPP(Ph)P-pln}(PMe_2Ph)$_2$] (**5**) exhibits too low values for nitrogen and carbon (cf. experimental section) indicating that decoordination of both the N_2 ligand and the coligand PMe_2Ph occurs. The instability of [Mo(N_2){prPP(Ph)P-pln}(PMe_2Ph)$_2$] (**5**) could also be observed in solution via NMR spectroscopy since we repeated the measurement of the same NMR sample after two weeks, showing that new signals had appeared and the amount of free coligand PMe_2Ph had increased (cf. SI, Figure S22).

In analogy to compound **3**, we also attempted to protonate [Mo(N_2){prPP(Ph)P-pln}(PMe_2Ph)$_2$] (**5**) by adding two equivalents of different acids {$HBAr^F{}_4$ and [LutH]$BAr^F{}_4$ with the non-coordinating anion $BAr^F{}_4^-$ = tetrakis[3,5-bis(trifluoromethyl)-phenyl]borate or [LutH]OTf with the coordinating anion TfO^-} to a solution of **5** in [D_8]THF. These experiments were performed in a young tube to investigate the reaction immediately by NMR spectroscopy. Nevertheless, only a decomposition of the molybdenum(0) mono(dinitrogen) complex [Mo(N_2){prPP(Ph)P-pln}(PMe_2Ph)$_2$] (**5**) was observed, which was ascribed to the fact that the monodentate phosphine ligands are substituted by, e.g., coordinating anions or hydrides.[66]

Conclusion

We established a new access to oligodentate ligands with phospholane end groups and demonstrated coordination of the tridentate ligand **prPP(Ph)P-pln** to molybdenum(III) centers as well as formation of molybdenum mono(dinitrogen) or bis(dinitrogen) complexes by sodium amalgam reduction of the molybdenum(III) precursors. The constitution of the final product was, however, found to strongly depend on the applied coligands. Using monodentate coligands, only a meridional coordination of **prPP(Ph)P-pln** and the formation of one isomer was observed. Using two equivalents of $PMePh_2$ as coligand, the reduction of [$MoBr_3${prPP(Ph)P-pln}] (**1-Br**) via sodium amalgam led to the bis(dinitrogen) complex [Mo(N_2)$_2${prPP(Ph)P-pln}($PMePh_2$)] (**3**), which could be converted into the hydrazido complex [Mo(NNH_2)(OTf){prPP(Ph)P-pln}($PMePh_2$)]OTf (**4**). Applying less sterically demanding PMe_2Ph as coligand the mono(dinitrogen) complex [Mo(N_2){prPP(Ph)P-pln}(PMe_2Ph)$_2$] (**5**) supported by the tridentate ligand **prPP(Ph)P-pln** was obtained which, however, could not be protonated.

If bidentate dppm was employed as a coligand in the described syntheses a mixture of isomers was formed whereby **prPP(Ph)P-pln** coordinates in a meridional or facial fashion. Because of the large amount of uncoordinated dppm found in the product, it appears that this ligand is only weakly bound in this type of complexes. Using less sterically demanding dmpm as coligand, however, no well-defined complex was obtained.

To conclude, we have presented the first molybdenum dinitrogen complexes supported by a tridentate ligand with phospholane end groups, employing lithium phospholanide as a useful and versatile building block for the synthesis of such multidentate ligands. Further studies will be devoted to explore the application of phospholane end groups in tripods or ligands of higher denticity such as pentadentate tetrapodal (pentaPod) ligands which we have recently employed in synthetic nitrogen fixation.[27]

Experimental Section

General Information: Commercially available starting materials were used as received. Water- and oxygen-sensitive reagents were handled in a M. Braun Labmaster 130 Glovebox under N_2. All syntheses were performed in dried solvents under a N_2 atmosphere by using Schlenk techniques. Solvents were dried with CaH_2 (dichloromethane, *n*-hexane, *n*-pentane), $LiAlH_4$ (THF, diethyl ether) or magnesium methoxide (methanol) under Ar and freshly distilled prior to use. [$MoCl_3(thf)_3$],[67] [$MoBr_3(thf)_3$],[68] [$MoI_3(thf)_3$],[69] ethyl phospholanate,[53] phenylphosphine[56,57] as well as bis(3-chloropropyl)-phenylphoshine[58] were prepared as described in the literature. Elemental analyses were performed using a EuroVector CHNSO-element analyzer (Euro EA 3000) or a vario MICRO cube (Co. Elementar Analysensysteme). Samples were burned in sealed tin containers in a stream of oxygen. NMR spectra were recorded with a Bruker Avance 400 Pulse Fourier Transform spectrometer operating at frequencies of 400.13 MHz (^1H), 376.46 MHz (^{19}F) 161.98 MHz (^{31}P), 155.51 MHz (^7Li) and 100.62 MHz (^{13}C). Referencing was performed either using the solvent residue signal (7.26 ppm for $CDCl_3$, 5.32 ppm for CD_2Cl_2, 3.58 ppm for [D_8]THF, 3.31 ppm for CD_3OD). ^7Li NMR spectra were referenced to LiCl in D_2O [$\delta(^7Li)$ = 0 ppm], ^{19}F NMR spectra were referenced to $CFCl_3$ in $CDCl_3$ [$\delta(^{19}F)$ = 0 ppm] and ^{31}P NMR spectra were referenced to H_3PO_4 85 % [$\delta(^{31}P)$ = 0 ppm] as substitutive standard. Infrared spectra were recorded on a Bruker Alpha FT-IR Spectrum with Platinum ATR setup. Solution-

phase IR spectroscopy was performed with a Bruker Vertex 70 spectrometer at a resolution of 2 cm^{-1}. Raman spectra were recorded at room temp. on a Bruker RAM II FT-Raman spectrometer using a liquid nitrogen cooled, highly sensitive Ge detector, 1064 nm radiation and 3 cm^{-1} resolution.

Single Crystal Structure Analysis of 1-Cl: Data collection was performed with an Imaging Plate Diffraction System (IPDS-2) from STOE A numerical absorption correction was performed (Tmin/max: 0.8061/0.8725). All non-hydrogen atoms were refined anisotropic. The C-H H atoms were positioned with idealized geometry and were refined isotropic with $U_{iso}(H) = 1.2\ U_{eq}(C)$ using a riding model. Selected crystal data and details of the structure refinement can be found in Table S1 and an ORTEP plot as well as lists with bond lengths and angles can be found in Figure S27 and Table S2.

CCDC 1955603 (for **1-Cl**) contains the supplementary crystallographic data for this paper. These data can be obtained free of charge from The Cambridge Crystallographic Data Centre.

Lithium Phospholanide (Li-Pln): To a solution of ethyl phospholanate (22.9 g, 155 mmol) in diethyl ether (30 mL) were added a solution of lithium aluminium hydride in diethyl ether (1 M, 353 mL, 353 mmol) within 2.5 h at 0 °C. The reaction mixture was stirred for 14 h at room temperature followed by a very slow addition of degassed water (13.5 mL), of a 15 % degassed sodium hydroxide solution (13.5 mL) and again of degassed water (40 mL) at 0 °C. It was stirred for 1 h at room temperature, the white precipitate was filtered and washed with diethyl ether (80 mL). Most of the diethyl ether was removed using a distilling link. Afterwards, the product **H-Pln** could be obtained via distillation (7×10^{-3} mbar, 0–70 °C). This extremely volatile liquid compound is difficult to handle and cannot be stored conveniently. Therefore, **H-Pln** was distilled directly in a solution of *n*-butyllithium in *n*-hexane (2.5 M, 56 mL, 140 mmol) which was cooled to –78 °C to obtain **Li-Pln**. It was stirred for 16 h at room temperature. The colorless precipitate was filtered, washed with 60 mL *n*-hexane and dried in vacuo. The product **Li-Pln** was obtained as colorless solid (4.05 g, 43.1 mmol, 28 %).

Note: The product contains a little amount of *n*-hexane. It wasn't possible to remove it completely by drying in vacuo.

Isolated H-Pln: Anal.: Because of the pyrophoric property no elemental analysis was possible. $^{31}P\{^1H\}$ NMR (161.98 MHz, [D_8]THF, 300 K): δ = –70.9 ppm. ^{1}H-NMR (400.13 MHz, [D_8]THF, 300 K): δ = 2.96–2.41 (dm, 1 H, $^1J_{PH}$ = 180.1 Hz, H-Pln), 1.95–1.85 (m, 2 H, CH_2), 1.81–1.67 (m, 4 H, CH_2), 1.48–1.33 (m, 2 H, CH_2) ppm.

Li-Pln: Anal.: Because of the pyrophoric property no elemental analysis was possible. $^{31}P\{^1H\}$ NMR (161.98 MHz, [D_8]THF, 300 K): δ = –92.1 (s, 1 P, Li-Pln) ppm. $^{31}P\{^1H\}$ NMR: (161.98 MHz, CD_3OD, 300 K): δ = –72.8 (t, 1 P, D-Pln) ppm. ^{1}H-NMR (400.13 MHz, [D_8]THF, 300 K): δ = 2.00–1.98 (m, 4 H, CH_2 (Li-Pln)), 1.68–1.67 (m, 4 H, CH_2 (Li-Pln)) ppm. ^{1}H-NMR (400.13 MHz, CD_3OD, 300 K): δ = 1.96–1.86 (m, 2 H, CH_2 (D-Pln)), 1.83–1.69 (m, 4 H, CH_2 (D-Pln)), 1.49–1.36 (m, 2 H, CH_2 (D-Pln)) ppm. $^{13}C\{^1H\}$ NMR (100.62 MHz, [D_8]THF, 300 K): δ = 33.2 (s, 2 C, CH_2 (Li-Pln)), 22.2 (d, J_{PC} = 23.9 Hz), 2 C (CH_2 (Li-Pln)) ppm. $^{13}C\{^1H\}$ NMR (101 MHz, CD_3OD, 300 K): δ = 31.2 (d, J_{PC} = 5.5 Hz, 2 C, CH_2 (D-Pln)), 20.3 (d, J_{PC} = 8.0 Hz, 2 C, CH_2 (D-Pln)) ppm. ^{7}Li-NMR (156 MHz, [D_8]THF, 300 K): δ = 1.60 (s, 1 Li) ppm.

Bis(3-phospholanopropyl)phenylphosphine [prPP(Ph)P-pln]: To a solution of bis(3-chloropropyl)phenylphosphine in THF (1.22 mM, 1.80 mL, 2.20 mmol) THF (15 mL) was added. To a solution of lithium phospholanide (436 mg, 2.20 mmol) in THF (15 mL) a solution of *n*-butyllithium in *n*-hexane (2.5 M, 4.60 mL, 11.5 mmol) was added. Within 30 min the lithium phospholanide/*n*-butyllithium solution was added to the bis(3-chlorpropyl)phenylphosphine solution at 0 °C. The solution was stirred for 60 h at room temperature. Degassed water (10 mL) was added and it was stirred for 30 min. The organic layer was separated with a syringe and the aqueous layer was extracted three times with diethyl ether (5 mL). The solvent was removed in vacuo. The residue was redissolved in dichloromethane (5 mL), filtered through basic aluminum oxide and washed with dichloromethane (50 mL) to give the product as colorless oil (735 mg, 2.00 mmol, 91 %). Anal.: $C_{20}H_{33}P_3$ (366.40): C 65.6, H 9.1; found C 65.6, H 9.4.$^{31}P\{^1H\}$ NMR: (161.98 MHz, $CDCl_3$, 300 K): δ = –25.5 (s, 1 P, PPh_2), –27.0 (s, 2 P, P_{Pln}) ppm. ^{1}H-NMR (400.13 MHz, $CDCl_3$, 300 K): δ = 7.52–7.46 (m, 2 H, CH_{phenyl}), 7.37–7.29 (m, 3 H, CH_{phenyl}), 1.84–1.71 (m, 8 H, CH_2), 1.70–1.57 (m, 8 H, CH_2), 1.53–1.32 (m, 12 H, CH_2) ppm. $^{13}C\{^1H\}$ NMR (100.62 MHz, $CDCl_3$, 300 K): δ = 138.5 (d, $^1J_{PC}$ = 14.8 Hz, 1 C, $C_{i,phenyl}$), 132.6 (d, J_{PC} = 18.7 Hz, 2 C, CH_{phenyl}), 128.9 (s, 1 C, CH_{phenyl}), 128.4 (d, J_{PC} = 6.9 Hz, 2 C, CH_{phenyl}), 30.7 (dd, J_{PC} = 11.0, 16.3 Hz, 2 C, *pr*-CH_2), 29.9 (t, J_{PC} = 11.6 Hz, 2 C, *pr*-CH_2), 27.9 (dd, J_{PC} = 1.3, 3.9 Hz, 4 C, $(CH_2)_{Pln}$), 26.0 (dd, J_{PC} = 9.1, 11.3 Hz, 4 C, $(CH_2)_{pln}$), 23.5 (dd, J_{PC} = 14.6, 16.5 Hz, 2 C, *pr*-CH_2) ppm. IR (ATR): $\tilde{\nu}$ = 3070 (w), 3049 (w), 2925 (s), 2884 (s), 2855 (s), 2349 (vw), 2324 (vw), 1867 (vw), 1806 (vw), 1589 (vw), 1570 (vw), 1484 (w), 1463 (sh), 1448 (m), 1433 (m), 1414 (br m), 1378 (w), 1338 (w), 1318 (w), 1301 (w), 1257 (w), 1239 (w), 1207 (vw), 1174 (vw), 1156 (w), 1107 (m), 1099 (sh), 1057 (w), 1053 (w), 1028 (m), 1000 (sh), 980 (w), 971 (w), 942 (br w), 865 (w), 837 (m), 803 (br m), 740 (s), 695 (s), 673 (m), 658 (m), 511 (sh), 486 (m), 469 (w), 447 (vw), 430 (vw), 403 (w) cm^{-1}.

[$MoCl_3${prPP(Ph)P-pln}] (1-Cl): The ligand **prPP(Ph)P-pln** (301 mg, 822 µmol) was dissolved in dichloromethane (4 mL). This solution was added to a suspension of [$MoCl_3$(thf)$_3$] (344 mg, 822 µmol), THF (4 mL) and dichloromethane (4 mL). After adding further THF (4 mL) it was stirred for 19 h at room temperature. The suspension was reduced in vacuo to a quantity of 20 mL, *n*-hexane (5 mL) was added, the precipitate was filtered, washed with THF (6 mL), *n*-hexane (6 mL) and diethyl ether (6 mL) and dried in vacuo. The product was obtained as yellow solid (192 mg, 338 µmol, 41 %). Anal. calcd. $C_{20}H_{33}Cl_3MoP_3$ (568.72): C 42.2, H 5.9; found C 42.1, H 5.8. IR (ATR): $\tilde{\nu}$ = 3056 (w), 2984 (sh), 2936 (w), 2904 (vw), 2895 (vw), 2860 (w), 2326 (br vw), 1982 (br vw), 1883 (br vw), 1810 (br w), 1588 (vw), 1573 (br vw), 1488 (br vw), 1460 (sh), 1447 (m), 1435 (m), 1420 (br m), 1404 (br m), 1389 (m), 1340 (w), 1316 (sh), 1304 (w), 1256 (br w), 1234 (sh), 1196 (sh), 1183 (w), 1158 (w), 1149 (w), 1133 (sh), 1117 (br m), 1100 (sh m), 1163 (m), 1147 (w), 1027 (m), 995 (m), 959 (sh), 951 (br m), 924 (w), 915 (br w), 855 (m), 830 (m), 804 (w), 788 (br w), 762 (m), 738 (s), 695 (s), 669 (m), 637 (m), 617 (w), 600 (w), 517 (m), 491 (s), 480 (sh), 450 (br w), 414 (m), 400 (w), 371 (w), 313 (s), 296 (s), 275 (s), 263 (sh) cm^{-1}.

[$MoBr_3${prPP(Ph)P-pln}] (1-Br): The ligand **prPP(Ph)P-pln** (401 mg, 1.09 mmol) was dissolved in THF (10 mL). This solution was added to [$MoBr_3$(thf)$_3$] (603 mg, 1.09 mmol) and further THF (10 mL) was added. It was stirred for 16 h at room temperature. The suspension was reduced to a quantity of 5 mL and diethyl ether (20 mL) was added. The precipitate was filtered, washed with *n*-hexane (20 mL) and diethyl ether (2 × 20 mL) and dried in vacuo. The product was obtained as yellow solid (422 mg, 601 µmol, 55 %). Anal. calcd. $C_{20}H_{33}Br_3MoP_3$ (702.08): C 34.2, H 4.7; found C 34.2, H 4.8. IR (ATR): $\tilde{\nu}$ = 3054 (w), 2932 (br m), 2893 (sh), 2858 (m), 2326 (vw), 1587 (vw), 1572 (vw), 1484 (w), 1456 (sh), 1446 (m), 1434 (m), 1410 (br m), 1392 (sh), 1340 (w), 1316 (sh), 1304 (w), 1255 (br w), 1239 (sh), 1181 (w), 1158 (w), 1134 (w), 1114 (m), 1102 (sh), 1062 (m), 1027 (m), 993 (m), 953 (m), 924 (w), 912 (w), 868 (sh), 852 (m), 830 (m), 806 (w), 787 (w), 763 (m), 743 (sh), 738 (m), 694 (s), 667 (m), 636 (m), 615 (vw), 512 (br m), 489 (br m), 480 (sh), 452 (vw), 415 (m), 373 (w), 355 (vw), 311 (br w), 302 (w), 279 (w), 247 (br s), 222 (br s), 206 (sh) cm^{-1}.

[MoI_3{prPP(Ph)P-pln}] (1-I): The ligand **prPP(Ph)P-pln** (400 mg, 1.09 mmol) was dissolved in THF (10 mL). This solution was added to [$MoI_3(thf)_3$] (750 mg, 1.08 mmol). After adding further THF (10 mL) it was stirred for 18 h at room temperature. The suspension was reduced in vacuo to a quantity of 5 mL, diethyl ether (20 mL) was added. The precipitate was filtered, washed with *n*-hexane (10 mL) and diethyl ether (2 × 20 mL) and dried in vacuo. The product was obtained as orange-brown solid (680 mg, 807 µmol, 74 %). Anal. calcd. $C_{20}H_{33}I_3MoP_3$ (843.08): C 28.5, H 4.0; found C 29.2, H 4.2. IR (ATR): $\tilde{\nu}$ = 3076 (vw), 3052 (vw), 3012 (vw), 2936 (m), 2898 (sh), 2847 (vw), 2352 (vw), 2325 (vw), 2291 (vw), 1984 (vw), 1931 (w), 1848 (br w), 1612 (br w), 1586 (w), 1571 (w), 1485 (w), 1446 (m), 1433 (m), 1409 (br m), 1400 (sh), 1341 (vw), 1320 (sh), 1302 (w), 1255 (br w), 1234 (sh), 1179 (w), 1159 (vw), 1129 (sh), 1112 (m), 1100 (sh), 1061 (m), 1027 (m), 992 (m), 987 (m), 953 (m), 923 (w), 912 (sh), 851 (m), 829 (w), 808 (vw), 788 (w), 760 (w), 739 (m), 693 (s), 669 (sh), 631 (m), 617 (w), 608 (w), 560 (vw), 551 (vw), 510 (sh), 486 (s), 466 (sh), 444 (vw), 413 (m), 405 (sh), 373 (vw), 349 (vw), 334 (vw), 307 (vw), 290 (vw), 275 (vw), 256 (vw), 233 (sh), 212 (br s), 201 (br s), 183 (m), 171 (sh), 162 (sh), 145 (m) cm^{-1}.

[$Mo(N_2)${prPP(Ph)P-pln}(dppm)] (*fac1*-2, *mer1*-2, *fac2*-2): To sodium amalgam (201 mg, 8.70 mmol Na, 2 mL of Hg) and THF (10 mL) was added a suspension of [MoI_3{prPP(Ph)P-pln}] (**1-I**, 330 mg, 390 µmol) and dppm (150 mg, 390 µmol) in THF (10 mL) and further THF (10 mL) was added. The reaction mixture was stirred for 23 h at room temperature under nitrogen atmosphere. The solution was decanted from amalgam, filtered and the solvent was evaporated by passing a steady stream of nitrogen over the solution at room temperature. The sticky oil was dissolved in diethyl ether (20 mL) and the solution was filtered through neutral aluminum oxide. The solvent was removed via a stream of nitrogen. The product was obtained as red oil. [$MoBr_3${prPP(Ph)P-pln}] (**1-Br**) can also be used as precursor. Anal.: For [$Mo(N_2)${prPP(Ph)P-pln}(dppm)] an elemental analysis could not be obtained because of the oily character of the material, the large amount of the coligand dppm, the presence of solvent (diethyl ether) and a side product. $^{31}P\{^1H\}$ NMR (161.98 MHz, C_6D_6, 300 K): *fac1*-[$Mo(N_2)${prPP(Ph)P-pln}-(dppm)]: δ = 31.9 (dddd, $^2J_{PP}$ = 95.7, 29.3, 22.8, 16.3 Hz, 1 P, P_a), 27.2 (dddd, $^2J_{PP}$ = 27.7, 22.8, 20.4, 17.4 Hz, 1 P, P_b), 19.5 (pseudo-"dtd", $^2J_{PP}$ = 91.3, 27.8, 27.7, 16.3 Hz, 1P, P_d), 12.7 (dddd, $^2J_{PP}$ = 95.7, 27.8, 17.4, 15.2 Hz, 1 P, P_g), 10.3 (dddd, $^2J_{PP}$ = 91.3, 29.3, 20.4, 15.2 Hz, 1 P, P_h) ppm. *mer1*-[$Mo(N_2)${prPP(Ph)P-pln}(dppm)]: δ = 22.0 (dddd, $^2J_{PP}$ = 38.8, 17.6, 14.8, 1.1 Hz, 2 P, $P_c/P_{c'}$), 17.9 (dddd, $^2J_{PP}$ = 94.5, 38.8, 38.8, 22.9 Hz, 1 P, P_e), 13.3 (dtd, $^2J_{PP}$ = 22.9, 14.8, 11.9 Hz, 1 P, P_f), 4.5 (dtd, $^2J_{PP}$ = 94.5, 17.6, 11.9 Hz, 1 P, P_i) ppm. *fac2*-[$Mo(N_2)${prPP(Ph)P-pln}(dppm)]: δ = 35.5 (AA', 2 P, P_{pln}), 19.6 (M, 1 P, P(Ph), this signal is covered by a signal of *fac1*-[$Mo(N_2)${prPP(Ph)P-pln}(dppm)]), 10.3 (XX', 2 P, PPh_2, this signal is covered by a signal of *fac1*-[$Mo(N_2)${prPP(Ph)P-pln}(dppm)]) ppm. Side product (*): δ = 15.5 (s) ppm. Uncoordinated dppm: δ = –23.0 (s, 2 P, PPh_2) ppm. IR (ATR): $\tilde{\nu}$ = 3138 (w), 3065 (sh), 3049 (br m), 3027 (sh), 3013 (w), 2997 (w), 2957 (sh), 2924 (br s), 2902 (sh), 2853 (s), 2800 (w), 1997 (m, NN), 1986 (w, NN), 1955 (sh, NN), 1929 (br s, NN), 1881 (br sh), 1841 (w), 1818 (vw), 1806 (vw), 1775 (w), 1660 (br w), 1618 (vw), 1582 (m), 1570 (m), 1547 (w), 1510 (vw), 1479 (m), 1449 (m), 1431 (vs), 1417 (sh), 1378 (br m), 1350 (w), 1324 (br w), 1303 (m), 1270 (sh), 1260 (m), 1233 (br sh), 1202 (w), 1180 (m), 1152 (m), 1105 (s), 1086 (br s), 1070 (s), 1048 (sh), 1024 (s), 999 (m), 986 (w), 871 (sh), 947 (br m), 911 (br m), 861 (m), 845 (br m), 823 (w), 806 (w), 789 (m), 740 (s), 690 (vs), 659 (sh), 614 (s), 552 (vw), 523 (s), 499 (vs), 475 (vs), 419 (s), 393 (s) cm^{-1}.

[$Mo(N_2)_2${prPP(Ph)P-pln}($PMePh_2$)] (3): To sodium amalgam (220 mg, 9.61 mmol Na, 2 mL of Hg) and THF (5 mL) was added a suspension of [$MoBr_3${prPP(Ph)P-pln}] (**1-Br**, 290 mg, 413 µmol) and $PMePh_2$ (83 mg, 413 µmol) in THF (5 mL). Further THF (15 mL) was added and the reaction mixture was stirred for 16 h at room temperature under nitrogen atmosphere. The solution was separated with a syringe from amalgam. After reducing the solvent in vacuo, the residue was dissolved in diethyl ether (10 mL) and the solution was filtered through neutral aluminum oxide. The solvent was reduced in vacuo to a quantity of 5 mL and methanol (5 mL) was added. The solvent was reduced in vacuo to a quantity of 5 mL again and further methanol (5 mL) was added to precipitate the product. The precipitate was filtered, washed with methanol (10 mL) and dried in vacuo to obtain the product as an orange solid (110 mg, 153 µmol, 37 %). Anal. calcd. $C_{33}H_{46}MoN_4$ (718.6): C 55.2, H 6.5, N 7.8 found C 55.0, H 6.8, N 2.0. The nitrogen value is too low because of the thermal instability of the product. $^{31}P\{^1H\}$ NMR (161.98 MHz, [D_8]THF, 300 K): δ = 25.0 (dd, $^2J_{Pa/a'Pc}$ = 29.0 Hz, $^2J_{Pa/a'Pb}$ = 18.0 Hz, 2 P, $P_{a/a'}$), 22.8 (dt, $^2J_{PbPc}$ = 100.8 Hz, $^2J_{Pa/a'Pb}$ = 18.0 Hz, 1 P, P_b), 18.0 (dt, $^2J_{PbPc}$ = 100.8 Hz, $^2J_{Pa/a'Pc}$ = 29.0 Hz, 1 P, P_c) ppm. ^{1}H-NMR (400.13 MHz, [D_8]THF, 300 K): δ = 7.81–7.77 (m, CH_{phenyl} ($PhPR_2$)), 7.58–7.54 (m, CH_{phenyl} ($PMePh_2$)), 7.45–7.41 (m, CH_{phenyl}), 7.40–7.32 (m, CH_{phenyl}), 7.29–7.25 (m, CH_{phenyl} ($PMePh_2$)), 7.21–7.16 (m, CH_{phenyl}), 2.11–1.15 [5xm, CH_2 (phospholane and propyl chains)], 2.06 (d, $^2J_{HP}$ = 4.2 Hz, CH_3 ($PMePh_2$)) ppm. $^{13}C\{^1H\}$ NMR (100.62 MHz, [D_8]THF, 300 K): δ = 146.7 (dt, J_{CP} = 1.9, 21.3 Hz, 2 C, C_{ipso} ($PMePh_2$)), 139.1 (d, J_{CP} = 18.3 Hz, 1 C, C_{ipso} ($PhPR_2$)), 132.8 (s, CH_{phenyl} ($PhPR_2$)), 131.9 (d, J_{CP} = 11.0 Hz, CH_{phenyl} ($PMePh_2$)), 129.1 (d, J_{CP} = 1.56 Hz, CH_{phenyl}), 128.9–128.8 (m, CH_{phenyl}), 128.5 (s, CH_{phenyl}), 128.5 (s, CH_{phenyl}), 128.4 (s, CH_{phenyl}), 128.3 (d, J_{CP} = 1.2 Hz, CH_{phenyl}), 31.4–31.2 (m, CH_2), 31.0 (m, CH_2), 30.3–30.1 (m, CH_2), 27.4 (s, CH_2), 27.1 (s, CH_2), 26.0 (t, J_{CP} = 7.4 Hz, CH_2), 20.7 (d, J_{CP} = 3.0 Hz, CH_2), 15.8 (d, J_{CP} = 17.8 Hz, CH_3 ($PMePh_2$)) ppm. IR (ATR): $\tilde{\nu}$ = 3073 (w), 3051 (w), 3019 (vw), 2998 (vw), 2961 (sh), 2918 (br m), 2903 (sh), 2853 (m), 2005 (w, *sym*-NN), 1924 (s, *asym*-NN), 1810 (sh), 1761 (vw), 1584 (w), 1570 (w), 1479 (w), 1463 (sh), 1447 (w), 1430 (m), 1418 (br m), 1377 (sh), 1326 (br sh), 1304 (w), 1278 (sh), 1260 (br m), 1175 (w), 1155 (w), 1144 (w), 1104 (m), 1089 (m), 1069 (w), 1055 (w), 1027 (m), 1017 (sh), 987 (w), 977 (sh), 949 (w), 922 (sh), 911 (w), 876 (br m), 863 (br m), 845 (m), 821 (sh), 803 (sh), 789 (m), 739 (m), 694 (s), 675 (s), 660 (m), 615 (br m), 550 (m), 503 (s), 492 (sh), 472 (s), 447 (m), 424 (sh) cm^{-1}. Raman: $\tilde{\nu}$ = 3056 (m), 2977 (sh), 2963 (sh), 2942 (sh), 2934 (sh), 2926 (sh), 2915 (m), 2901 (m), 2885 (sh), 2877 (sh), 2852 (sh), 2000 (s), 1930 (vw), 1587 (m), 1572 (w), 1451 (w), 1418 (br w), 1308 (br vw), 1257 (br vw), 1196 (sh), 1187 (w), 1159 (w), 1104 (br w), 1030 (m), 1000 (s), 964 (br vw), 917 (m), 870 (br w), 751 (br vw), 702 (vw), 683 (m), 670 (w), 645 (vw), 637 (vw), 619 (w), 494 (br w), 432 (vw), 415 (w) cm^{-1}.

[$Mo(NNH_2)(OTf)${prPP(Ph)P-pln}($PMePh_2$)]OTf (4): The complex [$Mo(N_2)_2${prPP(Ph)P-pln}($PMePh_2$)] (**3**, 20.0 mg, 27.8 µmol) was dissolved in 0.45 mL [D_8]Et_2O and 2.5 equivalents TfOH (6.1 µL, 69.5 µmol) were added. A grey solid precipitated wherefore the solvent was removed in vacuo and the residue was dissolved in CD_2Cl_2. The solution became red and 2.5 equiv. of. TfOH (6.1 µL, 69.5 µmol) were added. The solution was transferred in a young tube and characterized via NMR spectroscopy immediately. $^{31}P\{^1H\}$ NMR (161.98 MHz, CD_2Cl_2, 300 K): δ = 15.0 (dd, $^2J_{Pa/a'Pb}$ = 21.3 Hz, $^2J_{Pa/a'Pc}$ = 30.0 Hz, $P_{a/a'}$), 10.9 (dt, $^2J_{PbPa/a'}$ = 21.3 Hz, $^2J_{PbPc}$ = 135.6 Hz), 4.0 (dt, $^2J_{PcPa/a'}$ = 30.0 Hz, $^2J_{PcPb}$ = 135.6 Hz, P_c) ppm. ^{1}H-NMR (400.13 MHz, CD_2Cl_2, 300 K): δ = 8.9 (br s, N-H), 7.85–7.29 (6xm, CH_{phenyl}), 2.55 (d, *J* = 14.7 Hz), 2.21–1.43 (4xm) ppm. IR (ATR): $\tilde{\nu}$ = 3246 (w, N-H), 3103 (w, N-H), 3065 (w), 2999 (vw), 2951 (sh), 2942 (sh), 2926 (w), 2869 (w), 1589 (vw), 1485 (vw), 1454 (sh), 1440 (w), 1417 (w), 1327 (sh), 1304 (sh), 1282 (m), 1252 (sh), 1231 (s), 1200 (s), 1155 (s), 1114 (m), 1073 (vw), 1027 (s), 1013 (s), 979 (sh),

959 (sh), 938 (m), 923 (m), 889 (w), 863 (w), 850 (w), 834 (vw), 814 (w), 790 (w), 744 (m), 718 (vw), 690 (m), 629 (s), 585 (sh), 573 (m), 515 (s), 490 (m), 467 (w) cm^{-1}.

[Mo(N$_2$){prPP(Ph)P-pln}(PMe$_2$Ph)$_2$] (5): To sodium amalgam (200 mg, 8.70 mmol Na, 2 mL of Hg) and THF (5 mL) was added [MoBr$_3${prPP(Ph)P-pln}] (**1-Br**, 300 mg, 427 µmol) and further THF (25 mL). After adding the coligand PMe_2Ph (119 mg, 861 µmol), it was stirred for 16 h at room temperature under nitrogen atmosphere. The solution was separated by filtration from amalgam. After reducing the solvent in vacuo to a quantity of 10 mL, the solution was filtered through neutral aluminum oxide. The solvent was reduced in vacuo to a quantity of 5 mL and methanol (10 mL) was added. The precipitate was filtered, washed with methanol (10 mL) and dried in vacuo to obtain the product as a red solid (120 mg, 157 µmol, 37 %). Anal. calcd. $C_{36}H_{55}MoN_2P_5$ (766.68): N 3.7 C 56.4, H 7.2; found N 1.5, C 54.8, H 7.6. The C and N values are presumably too low due to decoordination of the N_2 ligand and the coligand PMe_2Ph. $^{31}P\{^1H\}$ NMR (161.98 MHz, [D$_8$]THF, 300 K): δ = 25.0 (ddd, $^2J_{PP}$ = 30.1, 19.3, 18.4 Hz, 2 P, $P_{a/a'}$), 15.3 (dtd, $^2J_{PP}$ = 85.9, 30.1, 13.6 Hz, 1 P, P_b), 9.4 (dtd, $^2J_{PP}$ = 19.3, 18.4, 13.6 Hz, 1 P, P_c), 3.7 ("dq"= dtd, $^2J_{PP}$ = 85.9, 19.3, 19.3 Hz, 1 P, P_d) ppm. ^{1}H-NMR (400.13 MHz, [D$_8$]THF, 300 K): δ = 7.65–7.63 (m, 2 H, CH_{ortho} (*Ph*PR$_2$)), 7.59–7.55 (m, 4 H, CH_{ortho} (PMe$_2$*Ph*)), 7.36–7.34 (m, 2 H, CH_{meta} (*Ph*PR$_2$)), 7.30–7.23 (m, 4 H, CH_{meta} (PMe$_2$*Ph*)), 7.22–7.12 (m, 3 H, CH_{para} (*Ph*PR$_2$, PMe$_2$*Ph*)), 2.41–2.33 (m, 2 H, CH_2), 1.89–1.77 (m, 8 H, CH_2), 1.68–1.57 (m, 2xd, 14 H, 4 × CH_2, 2 × CH_3), 1.55–1.34 (m, 14 H, CH_2),1.13–1.06 (m, 2 H, CH_2) ppm. $^{13}C\{^1H\}$ NMR (100.62 MHz, [D$_8$]THF, 300 K): δ = 153.7 (dt, J_{CP} = 2.5, 13.8 Hz, 1 C, C_{ipso} (PMe$_2$*Ph*)), 151.8 (dd, J_{CP} = 5.4, 17.0 Hz, 1 C, C_{ipso} (PMe$_2$*Ph*)), 138.6 (dd, J_{CP} = 3.7, 19.1 Hz, 1 C, C_{ipso} (*Ph*PR$_2$)), 132.4 (d, J_{PC} = 9.3 Hz, 2 C, C_{ortho} (*Ph*PR$_2$)), 131.1 (d, J_{CP} = 8.9 Hz, 2 C, C_{ortho} (PMe$_2$Ph)), 130.2 (d, J_{CP} = 8.5 Hz, 2 C, C_{ortho} (PMe$_2$*Ph*)), 128.5 (d, J_{CP} = 6.0 Hz, 2 C, C_{meta} (PMe$_2$*Ph*)), 128.2 (d, J_{CP} = 6.1 Hz, 2 C, C_{meta} (PMe$_2$*Ph*)), 127.7 (d, J_{CP} = 7.3 Hz, 2 C, C_{meta} (*Ph*PR$_2$)), 127.6 (dd, J_{CP} = 1.3 Hz, 1 C, C_{para} (*Ph*PR$_2$)), 127.4 (br s, 1 C, C_{para} (PMe$_2$*Ph*)), 127.3 (br s, 1 C, C_{para} (PMe$_2$*Ph*)), 37.3 (m, 2 C, CH_2), 34.2–34.0 (m, 2 C, CH_2), 32.2 (d, J_{CP} = 16.8 Hz, 2 C, CH_2), 28.2–28.0 (dm, 2 C, CH_3), 27.5 (s, 2 C, CH_2), 27.2 (s, 2 C, CH_2), 23.3–23.1 (m, 2 C, CH_2), 21.7 (d, 2 C, J_{CP} = 2.5 Hz), 21.6 (br s, 1 C, CH_3 (PMe$_2$Ph)), 21.4 (br s, 1 C, CH_3 (PMe$_2$Ph)) ppm. IR (ATR): $\tilde{\nu}$ = 3086 (vw), 3072 (vw), 3047 (w), 3017 (vw), 2995 (vw), 2959 (m), 2934 (sh), 2911 (m), 2889 (sh), 2853 (br m), 2804 (sh), 2008 (br w), 1944 (sh, NN), 1931 (s, NN), 1755 (vw), 1584 (w), 1569 (vw), 1487 (w), 1464 (vw), 1449 (w), 1430 (w), 1421 (sh), 1408 (w), 1375 (vw), 1319 (vw), 1306 (vw), 1287 (w), 1260 (m), 1181 (vw), 1156 (vw), 1145 (w), 1095 (br m), 1072 (sh), 1056 (m), 1019 (br m), 989 (sh), 972 (sh), 945 (sh), 929 (m), 923 (m), 889 (m), 863 (br w), 844 (br w), 817 (sh), 799 (br m), 773 (sh), 746 (sh), 739 (m), 704 (sh), 695 (br m), 657 (br m), 614 (m), 551 (vw), 519 (sh), 506 (m), 490 (m), 474 (m) cm^{-1}. Raman: $\tilde{\nu}$ = 3051 (m), 2970 (br sh), 2940 (m), 2908 (s), 2861 (sh), 2000 (vw), 1944 (m), 1933 (m), 1812 (vw), 1585 (m), 1568 (w), 1488 (vw), 1450 (w), 1423 (w), 1413 (w), 1400 (w), 1269 (w), 1251 (w), 1186 (w), 1156 (w), 1100 (br m), 1028 (m), 1001 (s), 931 (w), 920 (w), 895 (vw), 874 (vw), 747 (vw), 738 (vw), 706 (vw), 691 (w), 661 (m), 618 (m), 521 (vw), 498 (m), 488 (m), 442 (m) cm^{-1}.

Keywords: Nitrogen fixation · Phospholanes · Molybdenum · Synthesis design

[1] A. D. Allen, C. V. Senoff, *Chem. Commun.* **1965**, 621.
[2] a) Y. Nishibayashi, *Transition metal-dinitrogen complexes. Preparation and reactivity*, 1. Aufl., Wiley-VCH, Weinheim, Germany, **2019**; b) Y. Nishibayashi, *Dalton Trans.* **2018**, *47*, 11290; c) N. Stucke, B. M. Flöser, T. Weyrich, F. Tuczek, *Eur. J. Inorg. Chem.* **2018**, 1337; d) H. Broda, F. Tuczek, *Angew. Chem. Int. Ed.* **2014**, *53*, 632; *Angew. Chem.* **2014**, *126*, 644; e) M. D. Fryzuk, *Chem. Commun.* **2013**, *49*, 4866; f) M. D. Fryzuk, *Science* **2013**, *340*, 1530; g) Y. Tanabe, Y. Nishibayashi, *Coord. Chem. Rev.* **2013**, *257*, 2551; h) H. Broda, S. Hinrichsen, F. Tuczek, *Coord. Chem. Rev.* **2013**, *257*, 587.
[3] a) F. Mus, A. B. Alleman, N. Pence, L. C. Seefeldt, J. W. Peters, *Metallomics* **2018**, *10*, 523; b) N. S. Sickerman, K. Tanifuji, Y. Hu, M. W. Ribbe, *Chem. Eur. J.* **2017**, *23*, 12425; c) R. D. Milton, S. Abdellaoui, N. Khadka, D. R. Dean, D. Leech, L. C. Seefeldt, S. D. Minteer, *Energy Environ. Sci.* **2016**, *9*, 2550; d) B. M. Hoffman, D. Lukoyanov, Z.-Y. Yang, D. R. Dean, L. C. Seefeldt, *Chem. Rev.* **2014**, *114*, 4041; e) M. W. Ribbe, Y. Hu, K. O. Hodgson, B. Hedman, *Chem. Rev.* **2014**, *114*, 4063.
[4] a) K. M. Lancaster, M. Roemelt, P. Ettenhuber, Y. Hu, M. W. Ribbe, F. Neese, U. Bergmann, S. DeBeer, *Science* **2011**, *334*, 974; b) T. Spatzal, M. Aksoyoglu, L. Zhang, S. L. A. Andrade, E. Schleicher, S. Weber, D. C. Rees, O. Einsle, *Science* **2011**, *334*, 940.
[5] L. R. Doyle, A. J. Wooles, L. C. Jenkins, F. Tuna, E. J. L. McInnes, S. T. Liddle, *Angew. Chem. Int. Ed.* **2018**, *57*, 6314; *Angew. Chem.* **2018**, *130*, 6422.
[6] J. S. Anderson, J. Rittle, J. C. Peters, *Nature* **2013**, *501*, 84.
[7] K. Arashiba, Y. Miyake, Y. Nishibayashi, *Nat. Chem.* **2011**, *3*, 120.
[8] C. J. Pickett, K. S. Ryder, J. Talarmin, *J. Chem. Soc., Dalton Trans.* **1986**, 1453.
[9] D. V. Yandulov, R. R. Schrock, *Science* **2003**, *301*, 76.
[10] J. Chatt, A. J. Pearman, R. L. Richards, *Nature* **1975**, *253*, 39.
[11] a) M. Hidai, K. Tominari, Y. Uchida, *J. Am. Chem. Soc.* **1972**, *94*, 110; b) M. Hidai, K. Tominari, Y. Uchida, A. Misono, *J. Chem. Soc., D* **1969**, 1392.
[12] a) L. A. Wickramasinghe, T. Ogawa, R. R. Schrock, P. Müller, *J. Am. Chem. Soc.* **2017**, *139*, 9132; b) M. R. Reithofer, R. R. Schrock, P. Müller, *J. Am. Chem. Soc.* **2010**, *132*, 8349; c) R. R. Schrock, *Angew. Chem. Int. Ed.* **2008**, *47*, 5512; *Angew. Chem.* **2008**, *120*, 5594; d) R. R. Schrock, *Acc. Chem. Res.* **2005**, *38*, 955.
[13] S. Kuriyama, K. Arashiba, K. Nakajima, H. Tanaka, N. Kamaru, K. Yoshizawa, Y. Nishibayashi, *J. Am. Chem. Soc.* **2014**, *136*, 9719.
[14] K. Arashiba, E. Kinoshita, S. Kuriyama, A. Eizawa, K. Nakajima, H. Tanaka, K. Yoshizawa, Y. Nishibayashi, *J. Am. Chem. Soc.* **2015**, *137*, 5666.
[15] A. Eizawa, K. Arashiba, H. Tanaka, S. Kuriyama, Y. Matsuo, K. Nakajima, K. Yoshizawa, Y. Nishibayashi, *Nat. Commun.* **2017**, *8*, 14874.
[16] K. Arashiba, A. Eizawa, H. Tanaka, K. Nakajima, K. Yoshizawa, Y. Nishibayashi, *Bull. Chem. Soc. Jpn.* **2017**, *90*, 1111.
[17] Y. Ashida, K. Arashiba, K. Nakajima, Y. Nishibayashi, *Nature* **2019**, *568*, 536.
[18] Y. Ashida, K. Arashiba, H. Tanaka, A. Egi, K. Nakajima, K. Yoshizawa, Y. Nishibayashi, *Inorg. Chem.* **2019**, *58*, 8927.
[19] S. E. Creutz, J. C. Peters, *J. Am. Chem. Soc.* **2014**, *136*, 1105.
[20] N. X. Gu, G. Ung, J. C. Peters, *Chem. Commun.* **2019**, *55*, 5363.
[21] J. Higuchi, S. Kuriyama, A. Eizawa, K. Arashiba, K. Nakajima, Y. Nishibayashi, *Dalton Trans.* **2018**, *47*, 1117.
[22] Y. Sekiguchi, K. Arashiba, H. Tanaka, A. Eizawa, K. Nakajima, K. Yoshizawa, Y. Nishibayashi, *Angew. Chem. Int. Ed.* **2018**, *57*, 9064; *Angew. Chem.* **2018**, *130*, 9202.
[23] a) M. J. Chalkley, T. J. Del Castillo, B. D. Matson, J. C. Peters, *J. Am. Chem. Soc.* **2018**, *140*, 6122; b) J. Fajardo, J. C. Peters, *J. Am. Chem. Soc.* **2017**, *139*, 16105; c) M. J. Chalkley, T. J. Del Castillo, B. D. Matson, J. P. Roddy, J. C. Peters, *ACS Cent. Sci.* **2017**, *3*, 217; d) T. J. Del Castillo, N. B. Thompson, J. C. Peters, *J. Am. Chem. Soc.* **2016**, *138*, 5341.
[24] J. Krahmer, H. Broda, C. Näther, G. Peters, W. Thimm, F. Tuczek, *Eur. J. Inorg. Chem.* **2011**, 4377.
[25] L. Sönchksen, C. Gradert, J. Krahmer, C. Näther, F. Tuczek, *Inorg. Chem.* **2013**, *52*, 6576.
[26] H. Broda, J. Krahmer, F. Tuczek, *Eur. J. Inorg. Chem.* **2014**, 3564.
[27] S. Hinrichsen, A. Kindjajev, S. Adomeit, J. Krahmer, C. Näther, F. Tuczek, *Inorg. Chem.* **2016**, *55*, 8712.
[28] H. Broda, S. Hinrichsen, J. Krahmer, C. Näther, F. Tuczek, *Dalton Trans.* **2014**, *43*, 2007.
[29] S. Hinrichsen, A.-C. Schnoor, K. Grund, B. Flöser, A. Schlimm, C. Näther, J. Krahmer, F. Tuczek, *Dalton Trans.* **2016**, *45*, 14801.
[30] S. L. Foster, S. I. P. Bakovic, R. D. Duda, S. Maheshwari, R. D. Milton, S. D. Minteer, M. J. Janik, J. N. Renner, L. F. Greenlee, *Nat. Catal.* **2018**, *1*, 490.

[31] M. T. Mock, A. W. Pierpont, J. D. Egbert, M. O'Hagan, S. Chen, R. M. Bullock, W. G. Dougherty, W. S. Kassel, R. Rousseau, *Inorg. Chem.* **2015**, *54*, 4827.
[32] a) J. A. Bilbrey, A. H. Kazez, J. Locklin, W. D. Allen, *J. Comput. Chem.* **2013**, *34*, 1189; b) R. A. Baber, M. F. Haddow, A. J. Middleton, A. G. Orpen, P. G. Pringle, A. Haynes, G. L. Williams, R. Papp, *Organometallics* **2007**, *26*, 713; c) T. E. Müller, D. M. P. Mingos, *Trans. Met. Chem.* **1995**, *20*, 533.
[33] C. A. Tolman, *Chem. Rev.* **1977**, *77*, 313.
[34] M. J. Burk, *Acc. Chem. Res.* **2000**, *33*, 363.
[35] a) T. V. RajanBabu, Y.-Y. Yan, S. Shin, *J. Am. Chem. Soc.* **2001**, *123*, 10207; b) J. Holz, M. Quirmbach, U. Schmidt, D. Heller, R. Stürmer, A. Börner, *J. Org. Chem.* **1998**, *63*, 8031.
[36] a) M. J. Burk, J. E. Feaster, W. A. Nugent, R. L. Harlow, *J. Am. Chem. Soc.* **1993**, *115*, 10125; b) M. J. Burk, *J. Am. Chem. Soc.* **1991**, *113*, 8518; c) M. J. Burk, J. E. Feaster, R. L. Harlow, *Organometallics* **1990**, *9*, 2653.
[37] M. J. Burk, J. E. Feaster, R. L. Harlow, *Tetrahedron: Asymmetry* **1991**, *2*, 569.
[38] a) T. Clark, C. Landis, *Tetrahedron: Asymmetry* **2004**, *15*, 2123; b) J. Albrecht, U. Nagel, *Angew. Chem. Int. Ed.* **1996**, *35*, 407; *Angew. Chem.* **1996**, *108*, 444.
[39] M. J. Burk, R. L. Harlow, *Angew. Chem. Int. Ed.* **1990**, *29*, 1462; *Angew. Chem.* **1990**, *102*, 1511.
[40] J. Lloret Fillol, A. Kruckenberg, P. Scherl, H. Wadepohl, L. H. Gade, *Chem. Eur. J.* **2011**, *17*, 14047.
[41] L.-I. Rodríguez, T. Roth, J. Lloret Fillol, H. Wadepohl, L. H. Gade, *Chem. Eur. J.* **2012**, *18*, 3721.
[42] S. K. Gibbons, Z. Xu, R. P. Hughes, D. S. Glueck, A. L. Rheingold, *Organometallics* **2018**, *37*, 2159.
[43] a) R. Sablong, C. Newton, P. Dierkes, J. A. Osborn, *Tetrahedron Lett.* **1996**, *37*, 4933; b) T. Morimoto, N. Ando, K. Achiwa, *Synlett* **1996**, 1211.
[44] N. Grüger, L.-I. Rodríguez, H. Wadepohl, L. H. Gade, *Inorg. Chem.* **2013**, *52*, 2050.
[45] M. Garbe, K. Junge, S. Walker, Z. Wei, H. Jiao, A. Spannenberg, S. Bachmann, M. Scalone, M. Beller, *Angew. Chem. Int. Ed.* **2017**, *56*, 11237; *Angew. Chem.* **2017**, *129*, 11389.
[46] Y.-Y. Yan, T. V. RajanBabu, *Org. Lett.* **2000**, *2*, 199.
[47] L. Zhang, Y. Tang, Z. Han, K. Ding, *Angew. Chem. Int. Ed.* **2019**, *58*, 4973; *Angew. Chem.* **2019**, *131*, 5027.
[48] a) L. D. Field, I. P. Thomas, T. W. Hambley, P. Turner, *Inorg. Chem.* **1998**, *37*, 612; b) L. D. Field, I. P. Thomas, *Inorg. Chem.* **1996**, *34*, 2546.
[49] M. Streitberger, A. Schmied, E. Hey-Hawkins, *Inorg. Chem.* **2014**, *53*, 6794.
[50] M. Streitberger, A. Schmied, R. Hoy, E. Hey-Hawkins, *Dalton Trans.* **2016**, *45*, 11644.
[51] P. Boar, M. Streitberger, P. Lönnecke, E. Hey-Hawkins, *Inorg. Chem.* **2017**, *56*, 7285.
[52] V. A. D'yakonov, A. L. Makhamatkhanova, R. A. Agliullina, L. K. Dilmukhametova, T. V. Tyumkina, U. M. Dzhemilev, *Beilstein J. Org. Chem.* **2016**, *12*, 406.
[53] R. P. Polniaszek, A. L. Foster, *J. Org. Chem.* **1991**, *56*, 3137.
[54] R. A. Aitken, W. Masamba, N. J. Wilson, *Tetrahedron Lett.* **1997**, *38*, 8417.
[55] H. J. Reich, R. R. Dykstra, *Organometallics* **1994**, *13*, 4578.
[56] W. Kuchen, H. Buchwald, *Chem. Ber.* **1958**, *91*, 2296.
[57] U. Nagel, A. Bublewitz, *Chem. Ber.* **1992**, *125*, 1061.
[58] L. M. Green, D. W. Meek, *Polyhedron* **1990**, *9*, 35.
[59] B. Pietsch, L. Dahlenburg, *Inorg. Chim. Acta* **1988**, *145*, 195.
[60] Q. Liao, N. Saffon-Merceron, N. Mézailles, *ACS Catal.* **2015**, *5*, 6902.
[61] Q. Liao, N. Saffon-Merceron, N. Mézailles, *Angew. Chem. Int. Ed.* **2014**, *53*, 14206; *Angew. Chem.* **2014**, *126*, 14430.
[62] M. W. Anker, J. Chatt, G. J. Leigh, A. G. Wedd, *J. Chem. Soc., Dalton Trans.* **1975**, 2639.
[63] N. A. Buang, D. L. Hughes, N. Kashef, R. L. Richards, *J. Organomet. Chem.* **1987**, *323*, C47.
[64] a) M. Tamizmani, C. Sivasankar, *Eur. J. Inorg. Chem.* **2017**, 4239; b) B. M. Flöser, F. Tuczek, *Coord. Chem. Rev.* **2017**, *345*, 263; c) K. H. Horn, N. Böres, N. Lehnert, K. Mersmann, C. Näther, G. Peters, F. Tuczek, *Inorg. Chem.* **2005**, *44*, 3016; d) K. H. Horn, N. Lehnert, F. Tuczek, *Inorg. Chem.* **2003**, *42*, 1076; e) N. Lehnert, F. Tuczek, *Inorg. Chem.* **1999**, *38*, 1671; f) C. J. Pickett, *J. Biol. Inorg. Chem.* **1996**, *1*, 601; g) C. J. Pickett, J. Talarmin, *Nature* **1985**, *317*, 652.
[65] a) H. C. Wolf, *Z. Naturforsch. A* **1956**, 797; b) A. S. Davydov, *J. Exp. Theor. Phys.* **1948**, 210.
[66] a) T. A. George, L. Ma, S. N. Shailh, R. C. Tisdale, J. Zubieta, *Inorg. Chem.* **1990**, *29*, 4789; b) J. Chatt, A. J. Pearman, R. L. Richards, *J. Chem. Soc., Dalton Trans.* **1978**, 1766.
[67] F. Stoffelbach, D. Saurenz, R. Poli, *Eur. J. Inorg. Chem.* **2001**, 2699.
[68] B. E. Owens, R. Poli, A. L. Rheingold, *Inorg. Chem.* **1989**, *28*, 1456.
[69] a) F. A. Cotton, R. Poli, *Inorg. Chem.* **1987**, *26*, 1514; b) W. Strohmeier, *Chem. Ber.* **1961**, *94*, 3337.

Received: October 2, 2019

Phospholanes

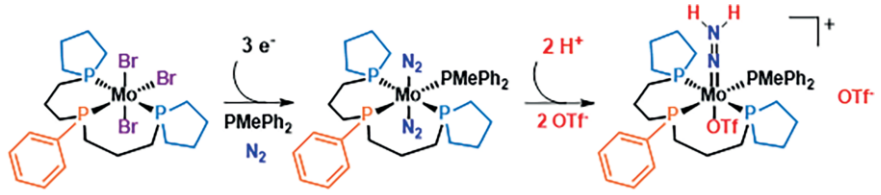

[$MoBr_3$(prPP(Ph)P-pln)]

The tridentate phosphine ligand **prPP(Ph)P-pln** with phospholane end groups is synthesized and used for the synthesis of MoX_3 (X = Cl, Br, I) precursors. Reduction in the presence of N_2 and either mono- or bidentate coligands led to molybdenum(0) mono- and bis(dinitrogen) complexes and subsequent protonation to a hydrazido complex.

DOI: 10.1002/ejic.201901068